Solar Phys (2015) 290:2827–2855
DOI 10.1007/s11207-015-0797-6

# Relations Between Microwave Bursts and Near-Earth High-Energy Proton Enhancements and Their Origin

**V.V. Grechnev[1] · V.I. Kiselev[1] · N.S. Meshalkina[1] · I.M. Chertok[2]**

Received: 26 May 2015 / Accepted: 30 September 2015 / Published online: 27 October 2015


**Abstract** We further study the relations between parameters of bursts at 35 GHz recorded with the *Nobeyama Radio Polarimeters* during 25 years and solar proton events (Grechnev *et al.* in *Publ. Astron. Soc. Japan* **65**, S4, 2013a). Here we address the relations between the microwave fluences at 35 GHz and near-Earth proton fluences above 100 MeV to find information on their sources and evaluate their diagnostic potential. The correlation between the microwave and proton fluences is pronouncedly higher than between their peak fluxes. This probably reflects a dependence of the total number of protons on the duration of the acceleration process. In events with strong flares, the correlation coefficients of high-energy proton fluences with microwave and soft X-ray fluences are higher than those with the speeds of coronal mass ejections. The results indicate a statistically larger contribution of flare processes to high-energy proton fluxes. Acceleration by shock waves seems to be less important at high energies in events associated with strong flares, although its contribution is probable and possibly prevails in weaker events. The probability of a detectable proton enhancement was found to directly depend on the peak flux, duration, and fluence of the 35 GHz burst, while the role of the Big Flare Syndrome might have been overestimated previously. Empirical diagnostic relations are proposed.

**Keywords** Solar proton events · Microwave bursts · Big flare syndrome · SEP diagnostics

✉ V.V. Grechnev
grechnev@iszf.irk.ru

V.I. Kiselev
valentin_kiselev@iszf.irk.ru

N.S. Meshalkina
nata@iszf.irk.ru

I.M. Chertok
ichertok@izmiran.ru

1 Institute of Solar-Terrestrial Physics SB RAS, Lermontov St. 126A, Irkutsk 664033, Russia

2 Pushkov Institute of Terrestrial Magnetism, Ionosphere and Radio Wave Propagation (IZMIRAN), Troitsk, Moscow 142190, Russia

## 1. Introduction

The problems of the origin of solar proton events (SPEs) and their diagnostics have been hotly debated for almost half a century. Two concepts of their origin are considered and even contrasted (see, *e.g.*, Kallenrode, 2003; Grechnev *et al.*, 2008; Aschwanden, 2012; Reames, 2013; Trottet *et al.*, 2015 for a review and references). The flare-acceleration concept relates the SPE sources to flare processes in coronal magnetic fields of active regions, manifested particularly in X-ray and microwave emissions. The shock-acceleration concept relates the major SPE sources to bow shocks driven by fast coronal mass ejections (CMEs).

There are convincing arguments in favor of both the flare and shock origin of SPEs. Gamma-rays concurrent with other flare emissions favor the hypothesis of acceleration of heavy particles in flares simultaneously with electrons (see, *e.g.*, Chupp and Ryan, 2009; Vilmer, MacKinnon, and Hurford, 2011). On the other hand, *in situ* measurements of the particle composition, such as the iron charge state, Fe/O ratio, and others appear to favor the shock-acceleration of ions at normal coronal temperatures (see, *e.g.*, Reames, 2013). We note that such measurements are limited to moderate ion energies, while the acceleration of heavier ions is indeed more effectively brought about by Fermi mechanisms operating in shock-acceleration. The apparent delay of the particle escape near the Sun (Reames, 2009, 2013) does not seem to be a reliable indication of their exceptional shock-acceleration because trapped flare-accelerated particles can escape from closed coronal structures after their delayed reconnection with open structures in the course of the CME expansion (Masson *et al.*, 2012; Grechnev *et al.*, 2013b). It is also possible that the alternative concepts are based on different observations that are subjected to selection effects.

The sources of the particle acceleration in flares and by shock waves are considered to be remote and independent of each other. The concepts of their origin are mainly based on hypotheses proposed in past decades, when opportunities of observing solar phenomena were much rarer than now. The well-known fact of a reduced proton productivity of short-duration events (referring to the soft X-ray (SXR) emission) led to the hypothesis that different acceleration mechanisms dominate in impulsive and gradual events (see, *e.g.*, Croom, 1971; Cliver *et al.*, 1989; Reames, 2009, 2013; and references therein).

However, recent observational studies have revealed a closer association between solar eruptions, flares, shock waves, and CMEs than previously assumed. It was found that the CME acceleration pulse occurs almost simultaneously with hard X-ray and microwave bursts (Zhang *et al.*, 2001; Temmer *et al.*, 2008, 2010). The helical component of the CME flux rope responsible for its acceleration is formed by reconnection that also causes a flare (Qiu *et al.*, 2007). A detailed quantitative correspondence has been established between the reconnected magnetic flux and the rate of the flare energy release (Miklenic, Veronig, and Vršnak, 2009). Most likely, a shock wave is typically excited by an erupting flux rope as an impulsive piston inside a developing CME during the rise phase of the hard X-ray and microwave bursts (Grechnev *et al.*, 2011, 2013a). Then the shock wave detaches from the piston and quasi-freely propagates afterward like a decelerating blast wave. Its transition to the bow-shock regime is possible later, if the CME is fast (Grechnev *et al.*, 2015). Thus, parameters of the CME and shock wave should be related to those of a corresponding flare, and the traditional contrasting of the acceleration in a flare and by a shock might be exaggerated. Some aspects of the correspondence between the parameters of flares, CMEs, shock waves, and SPEs have been stated by Nitta, Cliver, and Tylka (2003) and Gopalswamy *et al.* (2012).

Based on recent results, a correspondence between the parameters of SPEs and microwave bursts might be expected. The correlation between SPEs and strong high-frequency

radio bursts has been known for many decades (*e.g.*, Croom, 1971; Castelli and Barron, 1977; Akinian *et al.*, 1978; Cliver *et al.*, 1989, Melnikov *et al.*, 1991). Alternatively, Kahler (1982), advocating the shock-related origin of SPEs, explained this association by the Big Flare Syndrome (BFS), *i.e.*, a general correspondence between the energy release in an eruptive flare and its various manifestations. Thus, different flare parameters should correlate with each other regardless of any physical connection between them. The basic concept is clear, while the measure of the degree of correlation due to the BFS used by Kahler (1982) does not seem to be obvious. Assuming a single source for accelerated protons and heavier ions, he concluded that normal coronal temperatures of the ions ruled out the flare-related origin of the protons. Thus, the correlation with the thermal soft X-ray flux (1 – 8 Å) was considered as a measure of the BFS contribution. On the other hand, the mentioned reasons indicate the origins of protons in both flare-related and shock-related accelerators, whose efficiency can be largely different for different particles. It is difficult, if possible, to distinguish between different sources of the protons. For these reasons, Kahler (1982) might have somewhat overestimated the role of the BFS. A number of later studies that interpreted observational results in terms of traditional hypotheses apparently supported the shock-acceleration concept (*e.g.*, Tylka *et al.*, 2005; Rouillard *et al.*, 2012, and others), which has led to an underestimation of diagnostic opportunities of microwave bursts. Nevertheless, it seems worthwhile to analyze the relations between flare microwave bursts and SPEs, irrespective of their origin.

These relations were considered previously in a number of studies, but mostly at frequencies $< 17$ GHz (see, *e.g.*, Akinian *et al.*, 1978; Cliver *et al.*, 1989). These relatively low frequencies can belong to either the optically thin or thick branch of the gyrosynchrotron spectrum, which causes the ambiguity of the results and complicates their interpretation. This difficulty was overcome by Chertok, Grechnev, and Meshalkina (2009) through measuring microwave fluxes at two different frequencies.

Microwave emissions at higher frequencies in the optically thin regime seem to be most sensitive to large numbers of high-energy electrons gyrating in strong magnetic fields, being thus directly related to the energy release rate in the flare–CME formation process during its main (impulsive) phase. The frequency of 35 GHz is the highest at which stable long-term observations are available from the *Nobeyama Radio Polarimeters* (NoRP; Nakajima *et al.*, 1985). All of these circumstances determined our choice of the analyzed data.

In our previous study (Grechnev *et al.*, 2013b), we mainly analyzed the relations between peak fluxes at 35 GHz, $F_{35} \geq 10^3$ sfu (1 sfu $= 10^{-22}$ W m$^{-2}$ Hz$^{-1}$), recorded with NoRP since 1990 to 2012 on the one hand and peak fluxes of SPEs $> 100$ MeV, $J_{100}$, on the other hand. Most events showed a scattered direct tendency between the microwave and proton peak fluxes. Considerable SPEs were revealed even from eastern solar sources if the microwave bursts were strong enough.

A better correspondence might exist between some combinations of the time-integrals (fluences) of proton fluxes and microwave bursts (see, *e.g.*, Kahler, 1982; Chertok, 1990; Trottet *et al.*, 2015). In this study we consider these combinations.

An additional aspect of our analysis was inspired by a recent study of Trottet *et al.* (2015), who analyzed the correlations between proton fluxes in a range of 15 – 40 MeV and parameters characterizing flares and CMEs. Their analysis revealed significant correlations between the peak proton flux on the one hand and the start-to-peak SXR fluence and CME speed on the other hand. Neither the microwave fluence nor the SXR peak flux provided significant contribution to the total correlations. The results indicate that both flare-accelerated and shock-accelerated protons contribute to near-Earth fluxes in this energy range. Trottet *et al.* (2015) and Dierckxsens *et al.* (2015) revealed indications at the domination of shock-acceleration for protons with energies below 10 – 20 MeV and flare-acceleration for higher

energies, but the statistical significance of this finding was insufficient. Our data set allows us to verify this statement.

Our aim in this respect is not to advocate either of the concepts of the SPE origin. We try instead to understand how the results of our analysis as well as those of different studies (sometimes seemingly incompatible) might be reconciled with each other to form a probable consistent picture. In the course of our study, we endeavor to find what the 35 GHz radio bursts can tell us about SPEs, to reveal diagnostic opportunities of these radio bursts to promptly estimate a probable importance of a forthcoming high-energy SPE, and to highlight promising ways to further investigate the SPE problem.

Several studies considered a sample of SPEs selected by some criteria and analyzed parameters of responsible solar eruptive events. Our reverse approach misses many SPEs associated with weaker bursts, but this is natural for the diagnostic purposes and promises an understanding of how the parameters of microwave bursts are related to the proton productivity of solar events.

Section 2 considers statistical relations between the peak flux and the duration of the 35 GHz burst and the probability of a proton enhancement, as well as between the microwave and proton fluences. Section 3 analyzes correlations between proton fluences and parameters characterizing flares and shock waves, and examines which of these correlations are significant. Section 4 discusses the results and presents the main conclusions.

## 2. Statistical Analysis of Parameters of Microwave Bursts and Proton Fluxes > 100 MeV

### 2.1. Data

Data lists of microwave bursts recorded by NoRP are posted at http://solar.nro.nao.ac.jp/norp/html/event/. We considered all microwave bursts with peak flux densities at 35 GHz $F_{35} \geq 10^3$ sfu. This criterion has selected 104 bursts. We also searched for proton enhancements (*e.g.*, Kurt *et al.*, 2004) with peak fluxes $J_{100} > 10$ pfu (1 pfu = 1 particle $\mathrm{cm}^{-2}\,\mathrm{s}^{-1}\,\mathrm{sr}^{-1}$) to avoid missing large SPEs after weaker microwave bursts; this revealed seven additional events. Three of them were caused by backside sources, whose microwave emission could not reach Earth. No conclusions can be drawn about these events, and they were excluded from further analysis. Four large SPEs occurred after moderate microwave bursts with $F_{35} < 10^3$ sfu. Two of them caused ground level enhancements of cosmic ray intensity (GLEs): 2000-11-08, 2001-12-26 (GLE63), 2002-04-21, and 2012-05-17 (GLE71).

Automatically processed digital NoRP data in the XDR (IDLsave) format are accessible via ftp://solar-pub.nao.ac.jp/pub/nsro/norp/xdr/. The technique for accurately processing NoRP data and evaluating quantitative parameters of the bursts is described in Grechnev *et al.* (2013b). For each event we recalibrated the pre-burst level, which was often not perfect. This constant level was subtracted when we calculated the total microwave fluences. The contribution of the thermal bremsstrahlung was estimated from SXR GOES data for the four proton-abundant events. It was 42 % for the 2000-11-08 event, 31 % for 2012-05-17, 19 % for 2002-04-21, and 18 % for 2001-12-26. The thermal contribution to the remaining stronger bursts with peak fluxes $F_{35} \geq 1000$ sfu was neglected.

Digital data of GOES proton monitors are available at http://satdat.ngdc.noaa.gov/sem/goes/data/new_avg/. The total proton fluences were calculated for the integral proton channel $E_p > 100$ MeV for the whole time of a proton enhancement with subtraction of a constant background level. If an SPE overlapped with the decay phase of a preceding event, then the background was fit with an exponential function.

The data on events with the analyzed microwave bursts, corresponding proton enhancements, CMEs, and calculated parameters are presented in Table 1. The events are categorized according to their peak fluxes at 35 GHz, $F_{35}$, similar to the GOES classification. These are mX (microwave–eXtreme, $F_{35} > 10^4$ sfu), mS (microwave–Strong, $10^3$ sfu $< F_{35} < 10^4$ sfu), mM (microwave–Moderate, $10^2$ sfu $< F_{35} < 10^3$ sfu). The behind-the-limb events, whose microwave emission could not be detected, are categorized as mO (microwave–Occulted) events.

The list of events presented by Grechnev *et al.* (2013b) was supplemented with events since late 2012 to March 2015 and events 93 and 94, missing in the NoRP event list. A number of typos were corrected. The table is supplemented with the calculated total microwave and proton fluences, start-to-peak SXR fluences, and the CME speeds, if known. They were taken from the online CME catalog (Yashiro *et al.*, 2004; http://cdaw.gsfc.nasa.gov/CME_list/) containing the measurements from SOHO/LASCO data (Brueckner *et al.*, 1995). An atypical event 5 (SOL1991-05-18), previously assessed as a non-SPE, was reconsidered. This long-duration mX event was associated with an X2.8 flare, type IV and II bursts (*i.e.*, a CME and shock wave); thus, an SPE is expected in any case. Unlike an apparently well-connected position (N32W87), a related SPE had a long-lasting rise of more than half a day (Sladkova *et al.*, 1998) typical of events with far-east sources. Chertok, Grechnev, and Meshalkina (2009) assumed an unfavorable connection between its source and Earth that is supported by the occurrence of a geomagnetic storm on 17 – 19 May with Dst up to −105 nT (http://wdc.kugi.kyoto-u.ac.jp/dst_final/199105/index.html).

Column (1) of Table 1 presents the event number. Columns (2) and (3) show the date and time of the flare peak according to GOES reports. Columns (4) – (6) contain GOES class, start-to-peak SXR fluence, and flare coordinate.

Columns (7) – (9) list the half-height duration, peak intensity, and total microwave fluence at 35 GHz, $\Phi_{35}$. NoRP records at 35 GHz were absent or damaged for some events. In such cases, the value of $F_{35}$ was estimated by means of interpolation from the adjacent frequencies of 17 and 80 GHz and/or from the 34 GHz data of the *Nobeyama Radioheliograph* (NoRH; Nakajima *et al.*, 1994).

Columns (10) – (13) list parameters of near-Earth proton enhancements: the peak flux of protons with energies above 100 MeV, $J_{100}$; the total fluence, $\Phi_{100}$; the peak flux of protons with energies above 10 MeV, $J_{10}$; the index of the integral energy proton spectrum, $\delta_p = \log_{10}(J_{10}/J_{100})$, which was calculated from the peak fluxes of protons with different energies occurring at different times, thus attempting to take their velocity dispersion into account. The events marked in Column (13) with a superscript (a) were associated with GLEs. Column (14) presents the CME speed. Unknown or uncertain parameters are denoted by U. Confined flares are denoted by C.

The data from Table 1 are shown in Figure 1a, similar to a corresponding figure in Grechnev *et al.* (2013b). For clarity, solar events are categorized according to their heliolongitude, λ, into three intervals with boundaries of −30° and +20°, presented by the colored circles. The events without detectable proton fluxes are shown at the horizontal dotted line below, to reveal their amount. The majority of SPEs is grouped between the slanted lines $(F_{35}/1100)^2$ and $(F_{35}/13000)^2$ pfu, forming the main sequence. Four atypical proton-abundant mM events denoted by the black squares reside in the upper left part of the figure, much higher than the main sequence. The correlation coefficients between the logarithms of the peak values of the microwave and proton fluxes for all events, $\rho_{All}$, and separately for western events alone, with a heliolongitude $\lambda > 20°$, $\rho_{West}$, are shown in the upper part of the figure. The correlation for the western events is lower due to a considerable contribution from the four abundant events, all of which were located in the western hemisphere, while only 60 % of all SPEs had sources with $\lambda > 20°$.

**Table 1** Analyzed events.

| No | Date (yyyy-mm-dd) | Flare | | | | Microwave burst | | | Protons near Earth | | | | $V_{CME}$ |
|---|---|---|---|---|---|---|---|---|---|---|---|---|---|
| | | $T_{peak}$ | GOES class | $\Phi_{SXR}$ $10^{-3}$ J m$^{-2}$ | Position | $\Delta t_{35}$ min | $F_{35}$ $10^3$ sfu | $\Phi_{35}$ $10^5$ sfu s | $J_{100}$ pfu | $\Phi_{100}$ $10^3$ pfu s | $J_{10}$ pfu | $\delta_p$ km s$^{-1}$ | |
| (1) | (2) | (3) | (4) | (5) | (6) | (7) | (8) | (9) | (10) | (11) | (12) | (13) | (14) |
| mX events with extreme fluxes at 35 GHz ($F_{35} > 10^4$ sfu) | | | | | | | | | | | | | |
| 1 | 1990-04-15 | 02:55 | X1.4 | 190 | N32E54 | 66 | 20 | 202 | 0.04 | 4 | 9 | 2.35 | U |
| 2 | 1990-05-21 | 22:17 | X5.5 | 120 | N34W37 | 7 | 38 | 45 | 18 | 560 | 300 | 1.22[a] | U |
| 3 | 1991-03-22 | 22:45 | X9.4 | 200 | S26E28 | 2 | 122 | 65 | 55 | 1300 | 28000 | 2.70 | U |
| 4 | 1991-03-29 | 06:48 | X2.4 | 70 | S28W60 | 7 | 11 | 10 | 0 | 0 | 20 | U | U |
| 5 | 1991-05-18 | 05:46 | X2.8 | 470 | N32W87 | 26 | 21 | 143 | 0.05 | 3.3 | 7 | 2.14 | U |
| 6 | 1991-06-04 | 03:41 | X12 | 1060 | N30E60 | 15 | 130[b] | 470[b] | 2 | 90 | 50 | 1.40 | U |
| 7 | 1991-06-06 | 01:12 | X12 | 750 | N33E44 | 17 | 130[b] | 890[b] | 2.5 | 569 | 200 | 1.90 | U |
| 8 | 1991-06-09 | 01:40 | X10 | 310 | N34E04 | 7 | 74 | 87 | 1.2 | 17 | 80 | 1.82 | U |
| 9 | 1991-06-11 | 02:06 | X12 | 500 | N32W15 | 18 | 46 | 159 | 168 | 2200 | 3000 | 1.25[a] | U |
| 10 | 1991-10-24 | 02:41 | X2.1 | 35 | S15E60 | 0.6 | 34 | 6.4 | 0 | 0 | 0 | U | U |
| 11 | 1992-11-02 | 03:08 | X9.0 | 530 | S23W90 | 15 | 41 | 195 | 70 | 2900 | 800 | 1.06[a] | U |
| 12 | 2001-04-02 | 21:51 | X17 | 930 | N18W82 | 6 | 25 | 38 | 4.8 | 220 | 380 | 1.90 | 2505 |
| 13 | 2002-07-23 | 00:35 | X4.8 | 210 | S13E72 | 17 | 15 | 51 | 0 | 0 | 0 | U | 2285 |
| 14 | 2002-08-24 | 01:12 | X3.1 | 178 | S02W81 | 16 | 11 | 46 | 27 | 400 | 220 | 0.91[a] | 1913 |
| 15 | 2004-11-10 | 02:13 | X2.5 | 80 | N09W49 | 7[b] | 10[b] | 15[b] | 2 | 71 | 75 | 1.57 | 3387 |
| 16 | 2005-01-20 | 07:01 | X7.1 | 500 | N12W58 | 25 | 85 | 370 | 680 | 6400 | 1800 | 0.42[a] | 2800[c] |
| 17 | 2006-12-13 | 02:40 | X3.4 | 310 | S06W24 | 31 | 14 | 32 | 88 | 1900 | 695 | 0.89[a] | 1774 |
| 18 | 2012-03-07 | 00:24 | X5.4 | 310 | N17E15 | 80 | 11 | 136 | 67 | 5300 | 1500 | 1.35 | 2684 |
| 19 | 2012-07-06 | 23:08 | X1.1 | 12 | S15W63 | 3 | 17 | 12 | 0.27 | 7.2 | 22 | 1.91 | 1828 |
| 20 | 2014-02-25 | 00:49 | X4.9 | 110 | S12E82 | 16 | 48 | 76 | 0.8 | 102.5 | 19 | 1.38 | 2147 |

**Table 1** (*Continued.*)

| No | Date (yyyy-mm-dd) | Flare | | | | Microwave burst | | | Protons near Earth | | | | $V_{CME}$ |
|---|---|---|---|---|---|---|---|---|---|---|---|---|---|
| | | $T_{peak}$ | GOES class | $\Phi_{SXR}$ $10^{-3}$ J m$^{-2}$ | Position | $\Delta t_{35}$ min | $F_{35}$ $10^3$ sfu | $\Phi_{35}$ $10^5$ sfu s | $J_{100}$ pfu | $\Phi_{100}$ $10^3$ pfu s | $J_{10}$ pfu | $\delta_p$ km s$^{-1}$ | |
| (1) | (2) | (3) | (4) | (5) | (6) | (7) | (8) | (9) | (10) | (11) | (12) | (13) | (14) |
| mS events with strong fluxes at 35 GHz ($10^3$ sfu $< F_{35} < 10^4$ sfu) | | | | | | | | | | | | | |
| 21 | 1990-05-11 | 05:48 | X2.4 | 70 | N15E13 | 14 | 2.0 | 1.8 | 0 | 0 | 0 | U | U |
| 22 | 1990-05-21 | 01:25 | M4.8 | 20 | N33W30 | 7 | 1.3 | 0.6 | U | U | U | U | U |
| 23 | 1990-05-23 | 04:20 | M8.7 | 50 | N33W55 | 10 | 1.0 | 1.5 | 0 | 0 | 0 | U | U |
| 24 | 1990-06-10 | 07:27 | M2.3 | 7 | N10W10 | 3 | 1.0 | 0.8 | 0 | 0 | 0 | U | U |
| 25 | 1991-01-25 | 06:30 | X10 | 250 | S12E90 | 6 | 9.4 | 13 | 0.14 | 13 | 1 | 0.85 | U |
| 26 | 1991-03-05 | 23:26 | M6.2 | 7 | S23E79 | 2 | 1.4 | 0.6 | 0 | 0 | 0 | U | U |
| 27 | 1991-03-07 | 07:49 | X5.5 | 15 | S20E62 | 3 | 2.0 | 1.5 | 0.08 | 1 | 0.7 | 0.94 | U |
| 28 | 1991-03-13 | 08:04 | X1.3 | 40 | S11E43 | 2 | 3.6 | 0.9 | 0.03 | 0.2 | 4.6 | 2.18 | U |
| 29 | 1991-03-16 | 00:50 | X1.8 | 40 | S10E09 | 3 | 3.2 | 0.4 | 0 | 0 | 0 | U | U |
| 30 | 1991-03-16 | 21:56 | M6.0 | 20 | S09W04 | 4 | 1.6 | 0.2 | 0 | 0 | 0 | U | U |
| 31 | 1991-03-19 | 01:58 | M6.7 | 8 | S10W33 | 1 | 7.2 | 1.9 | 0 | 0 | 0 | U | U |
| 32 | 1991-03-21 | 23:43 | M5.4 | 17 | S25E40 | 3 | 7.2 | 3.4 | 0 | 0 | 0 | U | U |
| 33 | 1991-03-23 | 22:18 | M5.6 | 30 | S25E16 | 15 | 1.7 | 1.1 | U | U | U | U | U |
| 34 | 1991-03-25 | 00:22 | X1.1 | 50 | S26E01 | 11 | 3.9 | 8.8 | 0 | 0 | 0 | U | U |
| 35 | 1991-03-25 | 08:18 | X5.3 | 150 | S25W03 | 4 | 4.2 | 4.1 | 0.5 | 6 | 150 | 2.47 | U |
| 36 | 1991-05-16 | 06:54 | M8.9 | 60 | N30W56 | 9 | 8.0 | 11 | U | U | U | U | U |
| 37 | 1991-05-29 | 23:43 | X1.0 | 20 | N05E38 | 1 | 1.7 | 0.4 | U | U | 0.8 | U | U |
| 38 | 1991-06-30 | 03:01 | M5.0 | 20 | S06W19 | 0.8 | 2.0 | 0.2 | 0 | 0 | 0 | U | U |
| 39 | 1991-07-30 | 07:12 | M7.2 | 6 | N14W58 | 0.9 | 2.0 | 0.3 | 0 | 0 | 0 | U | U |
| 40 | 1991-07-31 | 00:53 | X2.3 | 70 | S17E11 | 5 | 1.6 | 1.6 | 0 | 0 | 0 | U | U |

**Table 1** (*Continued.*)

| No | Date (yyyy-mm-dd) | Flare | | | | Microwave burst | | | Protons near Earth | | | | $V_{CME}$ |
|---|---|---|---|---|---|---|---|---|---|---|---|---|---|
| | | $T_{peak}$ | GOES class | $\Phi_{SXR}$ $10^{-3}$ J m$^{-2}$ | Position | $\Delta t_{35}$ min | $F_{35}$ $10^3$ sfu | $\Phi_{35}$ $10^5$ sfu s | $J_{100}$ pfu | $\Phi_{100}$ $10^3$ pfu s | $J_{10}$ pfu | $\delta_p$ km s$^{-1}$ | |
| (1) | (2) | (3) | (4) | (5) | (6) | (7) | (8) | (9) | (10) | (11) | (12) | (13) | (14) |
| 41 | 1991-08-02 | 03:16 | X1.5 | 50 | N25E15 | 8 | 1.2 | 2.7 | 0 | 0 | 0 | U | U |
| 42 | 1991-08-03 | 01:23 | M2.9 | 2.6 | N24E05 | 3 | 2.8 | 0.8 | 0 | 0 | 0 | U | U |
| 43 | 1991-08-25 | 00:49 | X2.1 | 260 | N24E77 | 29 | 1.4 | 10 | 0.03 | 1.1 | 21 | 2.84 | U |
| 44 | 1991-10-27 | 05:49 | X6.1 | 150 | S13E15 | 6 | 8.8 | 13 | 0 | 0 | 40 | U | U |
| 45 | 1991-11-02 | 06:47 | M9.1 | 22 | S13W61 | 3 | 1.4 | 0.5 | 0 | 0 | 0.3 | U | U |
| 46 | 1991-11-15 | 22:38 | X1.5 | 50 | S13W19 | 4 | 1.5 | 1.2 | 0.28 | 2.6 | 1.1 | 0.59 | U |
| 47 | 1992-02-14 | 23:09 | M7.0 | 15 | S12E02 | 1 | 1.0 | 0.3 | 0 | 0 | 0 | U | U |
| 48 | 1992-02-27 | 08:11 | C2.6 | 0.2 | N03W05 | 0.6 | 1.0 | 0.1 | 0 | 0 | 0 | U | U |
| 49 | 1992-06-28 | 05:15 | X1.8 | 170 | N11W90 | 14 | 1.3 | 7.5 | 0.22 | 1.6 | 14 | 1.80 | U |
| 50 | 1994-01-16 | 23:25 | M6.1 | 30 | N07E71 | 9 | 1.2 | 1.1 | 0 | 0 | 0 | U | U |
| 51 | 1997-11-04 | 05:58 | X2.1 | 26 | S14W33 | 3 | 1.0 | 0.7 | 2.3 | 59 | 72 | 1.50 | 785 |
| 52 | 1998-08-08 | 03:17 | M3.0 | 2 | N14E72 | 0.7 | 2.0 | 0.5 | 0 | 0 | 0 | U | U |
| 53 | 1998-08-22 | 00:01 | M9.0 | 30 | N42E51 | 6 | 1.0 | 1.7 | U | U | 2.5 | U | U |
| 54 | 1998-11-22 | 06:42 | X3.7 | 100 | S27W82 | 7 | 6.7 | 5.5 | 0.22 | 1.5 | 4 | 1.26 | U |
| 55 | 1999-08-20 | 23:08 | M9.8 | 7 | S23E60 | 1 | 3.0 | 0.6 | 0 | 0 | 0 | U | 812 |
| 56 | 1999-12-28 | 00:48 | X4.5 | 100 | N23W47 | 2 | 2.2 | 1.2 | 0.1 | 0.5 | 0.5 | 0.69 | 672 |
| 57 | 2000-09-30 | 23:21 | X1.2 | 30 | N09W75 | 4 | 5.3 | 2.3 | 0 | 0 | 0 | U | C |
| 58 | 2000-11-24 | 05:02 | X2.0 | 38 | N19W05 | 2 | 9.3 | 5.6 | 0.58 | 32 | 8 | 1.13 | 1289 |
| 59 | 2001-03-10 | 04:05 | X6.7 | 7 | N26W42 | 1 | 1.7 | 0.3 | 0 | 0 | 0.2 | U | 819 |
| 60 | 2001-04-03 | 03:57 | X1.2 | 146 | S21E71 | 31 | 2.9 | 19 | 0 | 0 | U | U | 1613 |
| 61 | 2001-04-10 | 05:26 | X2.3 | 100 | S24W05 | 30 | 3.0 | 28 | 0.47 | 15 | 100 | 2.32 | 2411 |

**Table 1** (*Continued.*)

| No | Date (yyyy-mm-dd) | Flare | | | | Microwave burst | | | Protons near Earth | | | | $V_{CME}$ |
|---|---|---|---|---|---|---|---|---|---|---|---|---|---|
| | | $T_{peak}$ | GOES class | $\Phi_{SXR}$ $10^{-3}$ J m$^{-2}$ | Position | $\Delta t_{35}$ min | $F_{35}$ $10^3$ sfu | $\Phi_{35}$ $10^5$ sfu s | $J_{100}$ pfu | $\Phi_{100}$ $10^3$ pfu s | $J_{10}$ pfu | $\delta_p$ km s$^{-1}$ | |
| (1) | (2) | (3) | (4) | (5) | (6) | (7) | (8) | (9) | (10) | (11) | (12) | (13) | (14) |
| 62 | 2001-10-12 | 03:27 | C7.6 | 1 | N16E70 | 1 | 1.3 | 0.3 | 0 | 0 | 0 | U | U |
| 63 | 2001-10-25 | 05:21 | C5.2 | 0.4 | S19W17 | 1 | 1.2 | 0.3 | 0 | 0 | 1 | U | C |
| 64 | 2002-02-20 | 06:12 | M5.1 | 16 | N13W68 | 5 | 1.5 | 0.9 | 0.1 | 0.3 | 10 | 2.00 | 952 |
| 65 | 2002-07-18 | 03:37 | M2.2 | 5 | N19W27 | 2 | 1.4 | 0.3 | 0 | 0 | 0 | U | C |
| 66 | 2002-08-20 | 01:40 | M5.0 | 5 | S08W34 | 0.5 | 1.8 | 0.1 | 0 | 0 | 0 | U | 961 |
| 67 | 2002-08-21 | 01:41 | M1.4 | 2 | S10W47 | 1 | 1.3 | 0.1 | 0 | 0 | 0 | U | 400 |
| 68 | 2002-08-21 | 05:34 | X1.0 | 10 | S09W50 | 0.7 | 1.4 | 0.3 | 0 | 0 | 0 | U | 268 |
| 69 | 2003-04-26 | 00:58 | M2.1 | 2.2 | N20W65 | 2 | 2.2 | 0.4 | 0 | 0 | 0 | U | 690 |
| 70 | 2003-04-26 | 03:06 | M2.1 | 2.4 | N20W69 | 0.3 | 2.4 | 0.1 | 0 | 0 | 0 | U | 289 |
| 71 | 2003-05-28 | 00:27 | X3.6 | 130 | S08W22 | 14 | 3.5 | 10 | 0.15 | 2.6 | 121 | 2.90 | 1366 |
| 72 | 2003-05-29 | 01:05 | X1.2 | 40 | S07W31 | 12 | 1.2 | 3.4 | 0.03 | 1.3 | 2 | 1.82 | 1237 |
| 73 | 2003-05-31 | 02:29 | M9.3 | 21 | S06W60 | 8 | 3.5 | 13 | 0.8 | 16 | 27 | 1.53 | 1835 |
| 74 | 2003-06-15 | 23:56 | X1.3 | 70 | S07E80 | 8 | 1.9 | 5.8 | 0 | 0 | 0 | U | 2053 |
| 75 | 2003-06-17 | 22:55 | M6.8 | 40 | S08E58 | 23 | 1.8 | 1.5 | 0 | 0 | 0 | U | 1813 |
| 76 | 2003-10-24 | 02:54 | M7.6 | 70 | S19E72 | 32 | 3.9 | 28 | 0 | 0 | 0 | U | 1055 |
| 77 | 2003-10-26 | 06:54 | X1.2 | 160 | S17E42 | 62 | 3.6 | 20 | 0 | 0 | 0 | U | 1371 |
| 78 | 2004-01-06 | 06:29 | M5.8 | 15 | N05E89 | 8 | 1.0 | 2.3 | 0 | 0 | 0 | U | 1469 |
| 79 | 2004-01-07 | 04:04 | M4.5 | 23 | N02E82 | 9 | 1.8 | 4.4 | 0 | 0 | 0 | U | 1581 |
| 80 | 2004-07-16 | 02:06 | X1.3 | 25 | S10E39 | 5 | 1.5 | 1.1 | 0 | 0 | 0 | U | 154 |
| 81 | 2004-08-14 | 05:44 | M7.4 | 11 | S12W29 | 7 | 1.0 | 0.4 | 0 | 0 | 0 | U | 307 |
| 82 | 2004-10-30 | 06:18 | M4.2 | 7 | N13W21 | 7 | 1.3 | 0.7 | 0.04 | 0.3 | 0.9 | 1.35 | 422 |

**Table 1** (*Continued.*)

| No | Date (yyyy-mm-dd) | Flare | | | | Microwave burst | | | Protons near Earth | | | | $V_{CME}$ |
|---|---|---|---|---|---|---|---|---|---|---|---|---|---|
| | | $T_{peak}$ | GOES class | $\Phi_{SXR}$ $10^{-3}$ J m$^{-2}$ | Position | $\Delta t_{35}$ min | $F_{35}$ $10^3$ sfu | $\Phi_{35}$ $10^5$ sfu s | $J_{100}$ pfu | $\Phi_{100}$ $10^3$ pfu s | $J_{10}$ pfu | $\delta_p$ km s$^{-1}$ | |
| (1) | (2) | (3) | (4) | (5) | (6) | (7) | (8) | (9) | (10) | (11) | (12) | (13) | (14) |
| 83 | 2004-11-03 | 03:35 | M1.6 | 6 | N07E46 | 10 | 1.0 | 3.2 | 0 | 0 | 0.4 | U | 918 |
| 84 | 2005-01-01 | 00:31 | X1.7 | 40 | N04E35 | 6 | 1.7 | 3.0 | 0 | 0 | 0 | U | 832 |
| 85 | 2005-01-15 | 00:43 | X1.2 | 25 | N13E05 | 6 | 3.3 | 1.5 | 0 | 0 | 0 | U | C |
| 86 | 2005-07-30 | 06:35 | X1.3 | 100 | N11E58 | 27 | 1.2 | 5.1 | 0 | 0 | 0 | U | 1968 |
| 87 | 2005-08-25 | 04:44 | M6.4 | 10 | N08E82 | 5 | 4.3 | 5.1 | 0 | 0 | 0 | U | 1327 |
| 88 | 2005-09-13 | 23:22 | X1.7 | 33 | S11E10 | 6 | 5.0 | 1.3 | 0.05 | 1 | 200 | 3.6 | 999[e] |
| 89 | 2005-09-17 | 06:05 | M9.8 | 20 | S11W41 | 6 | 1.3 | 1.8 | 0 | 0 | 1.4 | U | C |
| 90 | 2010-06-12 | 00:57 | M2.0 | 4 | N24W47 | 2[b] | 4.0[b] | 2.7[b] | 0.05 | 0.26 | 0.9 | 1.26 | 486 |
| 91 | 2011-08-04 | 03:57 | M9.3 | 26 | N16W49 | 11 | 1.4 | 3.4 | 1.5 | 28 | 77 | 1.71 | 1315 |
| 92 | 2011-08-09 | 08:05 | X6.9 | 86 | N17W83 | 6 | 1.0 | 4.4 | 2.5 | 22 | 22 | 0.94 | 1610 |
| 93[d] | 2011-09-06 | 22:20 | X2.2 | 50 | N14W18 | 2 | 3.0 | 5.5 | 0.5 | 8.2 | 10 | 1.30 | 575 |
| 94[d] | 2011-09-07 | 22:37 | X1.7 | 44 | N14W28 | 2 | 1.0 | 4.6 | 0.05 | 1.3 | 10 | 2.30 | 792 |
| 95 | 2012-01-23 | 03:59 | M8.7 | 60 | N29W36 | 39 | 2.2 | 24 | 2.3 | 85 | 2700 | 3.07 | 2175 |
| 96 | 2012-10-23 | 03:17 | X1.8 | 40 | S13E58 | 3 | 4.4 | 1.5 | 0 | 0 | 0 | U | C |
| 97 | 2013-05-13 | 02:17 | X1.7 | 130 | N10E89 | 18 | 1.2 | 5.2 | 0 | 0 | 0 | U | 1270 |
| 98 | 2013-05-14 | 01:11 | X3.2 | 100 | N11E74 | 22 | 1.1 | 0.6 | 0.03 | 0.12 | 1 | 1.52 | 2625 |
| 99 | 2013-10-28 | 01:59 | X1.0 | 61 | N04W66 | 8 | 1.9 | 2.6 | 0.12 | 7 | 5 | 1.62 | 695 |
| 100 | 2013-11-08 | 04:26 | X1.1 | 20 | S44E86 | 4 | 4.0 | 3.0 | 0 | 0 | 0.7 | U | 497 |
| 101 | 2014-10-22 | 01:59 | M8.7 | 80 | S12E21 | 8 | 1.6 | 7.8 | 0 | 0 | 0 | U | C |
| 102 | 2014-10-30 | 00:37 | M1.3 | 20 | S14W81 | 1.1 | 1.4 | 0.2 | 0 | 0 | 0 | U | C |
| 103 | 2014-12-20 | 00:28 | X1.8 | 83 | S18W28 | 6 | 1.0 | 5.2 | 0 | 0 | 1.5 | U | U |

**Table 1** (*Continued.*)

| No | Date (yyyy-mm-dd) | Flare | | | | Microwave burst | | | Protons near Earth | | | | $V_{CME}$ |
|---|---|---|---|---|---|---|---|---|---|---|---|---|---|
| | | $T_{peak}$ | GOES class | $\Phi_{SXR}$ $10^{-3}$ J m$^{-2}$ | Position | $\Delta t_{35}$ min | $F_{35}$ $10^3$ sfu | $\Phi_{35}$ $10^5$ sfu s | $J_{100}$ pfu | $\Phi_{100}$ $10^3$ pfu s | $J_{10}$ pfu | $\delta_p$ km s$^{-1}$ | |
| (1) | (2) | (3) | (4) | (5) | (6) | (7) | (8) | (9) | (10) | (11) | (12) | (13) | (14) |
| 104 | 2015-03-10 | 03:24 | M5.1 | 12 | S16E34 | 4.2 | 2.0 | 0.5 | 0 | 0 | 0 | U | U |
| mM events with strong proton fluxes ($J_{100} > 10$ pfu, $10^2$ sfu $< F_{35} < 10^3$ sfu) | | | | | | | | | | | | | |
| 105 | 2000-11-08 | 23:28 | M7.8 | 66 | N10W75 | 53 | 0.09 | 2.1 | 320 | 13000 | 14000 | 1.64 | 1738 |
| 106 | 2001-12-26 | 05:40 | M7.1 | 110 | N08W54 | 26 | 0.78 | 8.2 | 47 | 600 | 700 | 1.17[a] | 1446 |
| 107 | 2002-04-21 | 01:51 | X1.5 | 280 | S14W84 | 120 | 0.5[b] | 7.2[b] | 20 | 1500 | 2000 | 2.0 | 2393 |
| 108 | 2012-05-17 | 01:47 | M5.1 | 31 | N09W74 | 17 | 0.2 | 1.7 | 18 | 305 | 230 | 1.11[a] | 1582 |
| mO backside events with strong proton fluxes ($J_{100} > 10$ pfu) | | | | | | | | | | | | | |
| 109 | 1990-05-28 | 04:33 | U | 0 | N36W120 | U | U | U | 4.5 | 295 | 44 | 0.99[a] | U |
| 110 | 2001-04-18 | 02:14 | C2.2 | 45 | S20W115 | U | U | U | 12 | 270 | 230 | 1.28[a] | 2465 |
| 111 | 2001-08-15 | 23:50 | U | 0 | N01W120 | U | U | U | 27 | 670 | 470 | 1.24 | 1575 |

[a]GLE event.

[b]Estimated from different data.

[c]A compromise between the estimates of Gopalswamy *et al.* (2005) and Grechnev *et al.* (2008).

[d]Missing in the NoRP event list.

[e]Excluded from the analysis because of overlap with a preceding event.

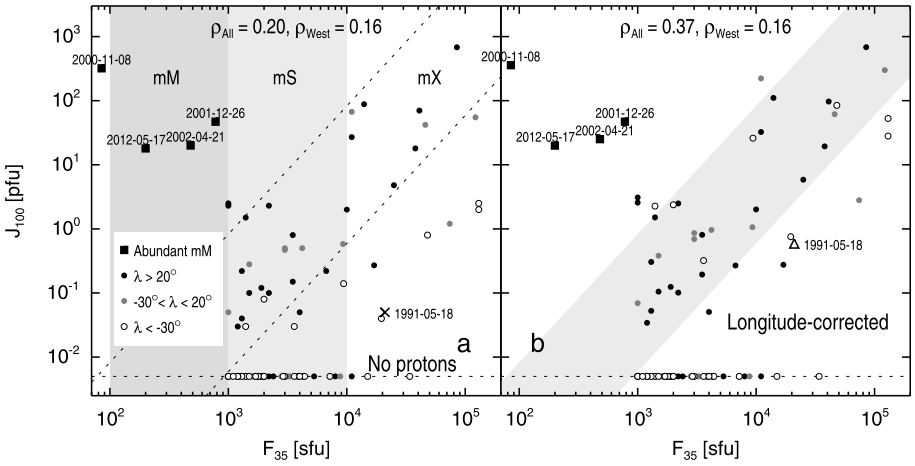


**Figure 1** Peak fluxes of > 100 MeV protons versus peak microwave fluxes at 35 GHz: (a) actual values and (b) with a positional correction. The longitude of the solar source for each data point is coded by the symbols explained in the legend in panel (a). The filled squares denote the mM events with atypically high SPEs. The 64 events without detectable proton fluxes falling outside the plot region are schematically presented along the horizontal dotted line below. The Pearson correlation coefficients specified in each panel were calculated separately for all 44 proton events ($\rho_{\rm All}$) and for 26 western proton events alone ($\rho_{\rm West}$). The slanted dotted lines, $(F_{35}/13000)^2$ and $(F_{35}/1100)^2$, in panel (a) and the corresponding shading in panel (b) enclose the majority of data points (main sequence), indicating a direct relation between the observed $F_{35}$ and $J_{100}$. (Updated plots from Grechnev *et al.*, 2013b).

Following Kahler (1982), we show in Figure 1b the same events, but with a correction $\exp\{[(\lambda - 54^\circ)/63]^2\}$ for the longitudinal dependence of > 100 MeV protons (Belov, 2009). This dependence is similar to the result of Lario *et al.* (2013), which was obtained for protons in an energy range of 25 – 53 MeV. The correction was formally applied to all events, including western events. The strongest effect of the correction is for far-eastern events (open circles), and a somewhat weaker effect is for moderately eastern events (gray filled circles). The usage of the longitudinal correction increases the correlation for the whole ensemble of events by 70 %. We therefore applied this correction in the subsequent analysis to all parameters of proton enhancements, even if their solar sources had western locations. Since this correction is uncertain, we additionally considered the correlation coefficients for western events alone.

It is not obvious how to handle the atypical event 5. This is an outlier with its actual longitude (the slanted cross in Figure 1a). According to its properties, event 5 should be handled in a way similar to the eastern events, but a suitable correction is unknown. As a tolerable, but practically inappropriate compromise, we handled this event as if it had a mid-eastern longitude of E45. The corresponding triangle in Figure 1b shows that this correction is not excessive.

All of the calculated correlation coefficients and regression parameters refer to logarithms of analyzed quantities rather than actual values because of their wide ranges. This way of linearization allows using the linear correlation analysis that is widely applied in many studies. On the other hand, logarithms of zero values are infinite, which requires a separate analysis of these terms. In addition, applying linear statistical methods to logarithms inevitably results in biased estimates due to the strong nonlinearity. Thus, the usage of the logarithmic scale is a necessary compromise, which allows comparing and quantifying statistical trends of an analyzed quantity on various parameters, but it is not mathematically rigorous.

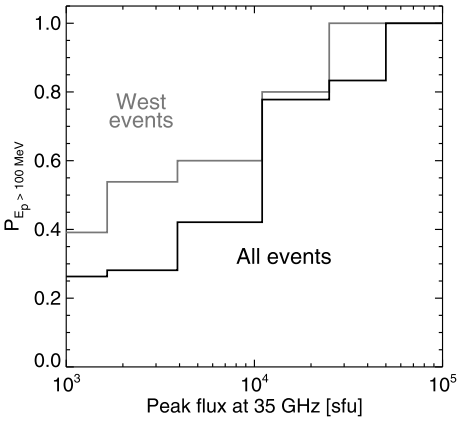


**Figure 2** Probability of a near-Earth proton enhancement with $E_P > 100$ MeV *vs.* peak flux of the 35 GHz burst irrespective of the burst duration or the position of a solar source.

## 2.2. Peak Flux at 35 GHz and the Probability of a High-Energy SPE

The percentage of SPEs associated with mX bursts is 90 %. Protons > 100 MeV were observed in 85 % of the mX events. GLEs occurred after 30 % of the mX events; in addition to the mX events, GLEs only occurred after two abundant mM events and two far-side mO events. The probability of a proton enhancement after an mS burst is considerably lower, 52 % for $E_p > 10$ MeV and 35 % for $E_p > 100$ MeV. None of the mS events produced a GLE.

It is difficult to evaluate the probability of SPEs after mM bursts because of their large number (270) and insufficient accuracy of the software, which calculates the parameters of the bursts posted at the NoRP website. An accurate processing of about 600 events is needed for a correct evaluation of the probability. Instead of this, we roughly estimated the upper and lower boundaries for the probability, using these lists and a catalog of SPEs presented at http://umbra.nascom.nasa.gov/SEP/. The total number of proton events with $J_{10} > 10$ pfu in the catalog from 1990 to March 2015, whose solar sources fell into the observing time in Nobeyama or were uncertain, was 70. Protons > 100 MeV were not observed in all of these events. Proceeding from the number of events in the catalogs, the probability of > 10 MeV SPEs after mM bursts was estimated to be within (8 – 23) %. The probability of high-energy SPEs after mM bursts was somewhat lower.

Figure 2 presents a more detailed probability distribution of high-energy SPEs depending on the 35 GHz peak flux, $F_{35}$. The shape of the histogram is sensitive to the bins because of a relatively small number of events. The intervals were chosen to reach a possibly larger number of bins, keeping the histogram monotonic. After a microwave burst with a peak flux of $F_{35} \approx 10^3$ sfu, the SPE probability is 25 – 40 %. With an increase of $F_{35}$, the probability increases, approaching 100 % for $F_{35} > 5 \times 10^4$ sfu. The SPE probability after a western solar event is 10 – 20 % higher than the probability averaged over the whole set of events.

Thus, the probability of a proton enhancement directly depends on the peak flux of the microwave burst at 35 GHz. This fact is consistent with a result of Dierckxsens *et al.* (2015) and the conclusion of Grechnev *et al.* (2013b) that a powerful microwave burst indicates a large proton event with a hard spectrum, up to a GLE, if the duration of the burst is long. The latter condition is analyzed in the next section.

### 2.3. The Role of the Duration of a Microwave Burst

The distribution of SPE peak fluxes *vs.* the peak fluxes of the microwave bursts, and their durations obtained by Grechnev *et al.* (2013b) confirmed the well-known reduced proton productivity of short-duration events. However, this distribution does not resemble two separate clusters with different durations that could be expected as a manifestation of two different acceleration mechanisms. Instead, a general, although scattered, tendency is surmised. To find the reasons for the reduced proton productivity of impulsive events, we first consider the properties of the distribution of microwave bursts on their duration, and in the next section we analyze the correlations between various combinations of the peak values and fluences of microwave bursts and proton enhancements.

The events without detectable proton fluxes are presented along the horizontal dotted line at the bottom of Figure 1. The half-height durations of the corresponding microwave bursts range from 0.3 to 62 min with an average of 7.7 min ($\sigma_n = 10.2$ min). The durations of SPE-related events range from 2 to 80 min with an average of 14.1 min ($\sigma_p = 16.5$ min). The difference in the durations by a factor of 1.8 appears only in averages, and its significance is questionable.

We consider the properties of the distributions of microwave bursts with $F_{35} \geq 10^3$ sfu on their durations for SPE-related and non-SPE-related events separately irrespective of their other parameters. The histograms of these distributions calculated in a straightforward way are inconclusive because of the relatively small number of events. We used for the analysis a different way of calculating the integral probability distribution, $P(\Delta t \leq t)$. It is an antiderivative of the histogram with a maximum normalized to unity and characterizes the probability of an event, if its duration $\Delta t$ does not exceed a value of $t$.

The solid histogram-like line in Figure 3a presents the integral probability distribution for SPE-related microwave bursts depending on their duration. This distribution in the linear and logarithmic representations seems to be similar to the error function, $\mathrm{erf}(t/\tau)$, indicating that the duration distribution is close to normal. The derivative of the integral distribution $P(\Delta t \leq t) = \mathrm{erf}(t/\tau)$ is a probability density function, which is known to be a Gaussian centered at zero, $2\exp\{-(t/\tau)^2\}/(\tau\sqrt{\pi})$. By minimizing the difference between the actual distribution and the fit, we have found $\tau_p = 18.3$ min, which characterizes a typical duration of a SPE-related microwave burst. The corresponding fitting functions are shown by the dotted lines in Figures 3a and 3b.

The character of the duration distribution for non-SPE-related events turned out to be the same (Gaussian centered at zero), but with a lesser width, $\tau_n = 9.9$ min (Figures 3c and 3d). The fit is shown by the dashed line. For comparison, the gray dotted line in Figure 3d is the fit of the distribution for proton events. The ratio of the widths of the distributions for proton and non-proton events, $\tau_p/\tau_n = 1.8$, corresponds to the ratio of their actual average durations.

The calculated ratio of the probabilities of proton and non-proton events in Figure 3d is $P_p/P_n = \tau_p/\tau_n \exp\{{t_{35}}^2(1/\tau_p^2 - 1/\tau_n^2)\}$. If the duration of a microwave burst, $t_{35}$, is known, then the probability of a proton enhancement, $P_p(t_{35})$, can be estimated as

$$P_p(t_{35}) = 1/(P_p/P_n + 1) = \left(\tau_p/\tau_n \exp\left\{t_{35}^2\left(1/\tau_p^2 - 1/\tau_n^2\right)\right\} + 1\right)^{-1}. \quad (1)$$

With the parameters found for the analyzed set of events, this equation gives an estimate of 52 %. SPEs occurred after 41 out of 103 microwave bursts with fluxes $F_{35} \geq 10^3$ sfu, *i.e.*, in $\approx$40 % of the events. The calculated probability for proton events *vs.* the duration of the 35 GHz burst is shown in Figure 3e. The vertical dash-dotted line in Figures 3d and 3e

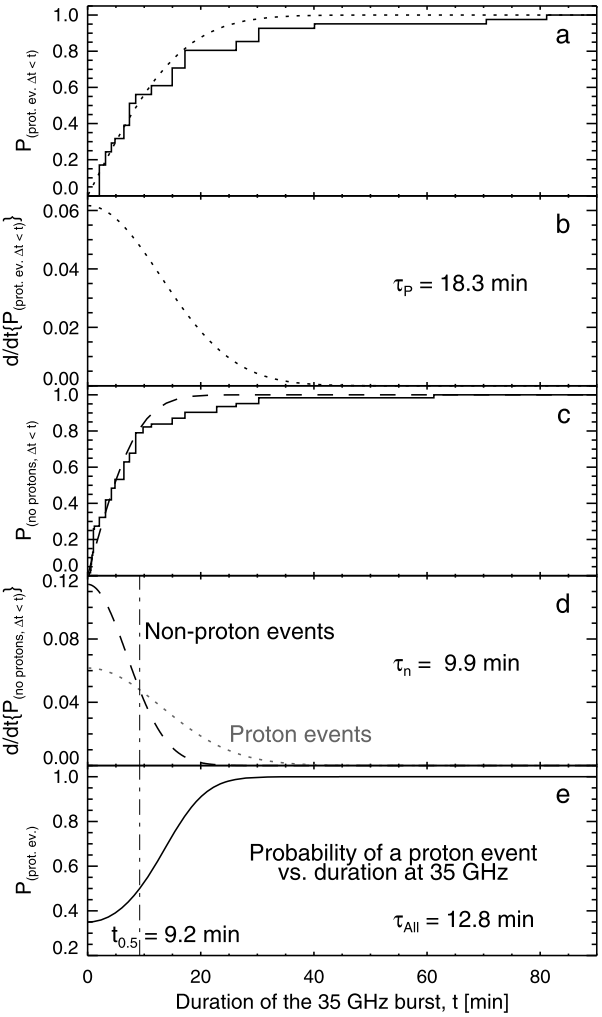


**Figure 3** Probability distributions of microwave bursts with peak fluxes $F_{35} \geq 10^3$ sfu on their durations. (a) Integral and (b) differential probability distributions for SPE-related events; (c) and (d) same for non-SPE-related events; (e) probability of a proton enhancement depending on the duration of the microwave burst. The histogram-style lines represent actual distributions, and the dotted curve shows the analytic fit. The gray dotted curve in panel (d) corresponds to the analytic fit in panel (b). The vertical dash-dotted line in panels (d) and (e) corresponds to the 50 % probability ($t_{35} = 9.2$ minutes).

denotes the burst duration of $t_{0.5} = 9.2$ min, at which the distribution functions of the proton and non-proton events are equal, which corresponds to a probability of 0.5. According to Figure 3e, if the peak flux of the 35 GHz burst exceeds $10^3$ sfu and its duration exceeds 30 min, then the SPE probability is almost 100 %.

The identity of the distribution functions for SPE-related and non-SPE-related events indicates the absence of essential differences between these classes of the events manifesting in their durations. The duration distribution of the whole set of microwave bursts, including both proton and non-proton events, is also similar to the normal distribution with $\tau_{All} = 12.8$ min. This distribution is not associated in any way with the proton productivity of the events, being an intrinsic characteristic of microwave bursts. A probable reason for the different widths of the distributions, $\tau_n < \tau_{All} < \tau_p$, is the sensitivity of the detectors that measure the proton fluxes in the Earth orbit against the radiation background. The decrease of the SPE peak due to the velocity dispersion of the proton bunch in the interplanetary space and other propagation effects is particularly strong if the bunch has a short duration.

The velocity dispersion (SPE rise) time for $> 100$ MeV protons can be roughly estimated as the difference between the straight Sun–Earth propagation times of the 100 MeV and relativistic protons, $t_{\rm D} \approx 1$ AU $\times (1/v - 1/c) = 1$ AU$/c \times (1/\sqrt{1 - 1/(E/m_{\rm p} + 1)^2} - 1) \approx 11$ min, with $E = 100$ MeV, $v$, and $m_{\rm p}$ being the kinetic energy, velocity, and the rest mass of protons; $c$ is the speed of light. A high-energy rollover of the proton spectrum decreases $t_{\rm D}$, while the actual path length, including the Parker spiral and particularities of the propagation in the interplanetary space, increases $t_{\rm D}$. Thus, $t_{\rm D} \sim t_{\rm n}$, consistent with our assumption. Similar reasons might also control the dependence of the SPE probability on the peak of the microwave burst shown in Figure 2.

The absence of two different clusters in the durations of the events, the absence of characteristic durations of the 35 GHz bursts in the events with protons and without them, and, instead, the same shapes of their distributions with most probable zero durations are not consistent with the two distinct classes of impulsive and gradual events. Therefore, a possible reason for the dependence of the number of high-energy protons on the duration of the event cannot be the difference in the particle acceleration mechanisms, but the duration of the acceleration process, on which the proton fluence should be directly dependent in any case. It also seems reasonable to consider the microwave fluence in addition to the peak flux. The fluence is an energy characteristic of the microwave emission throughout the flare, while the peak flux characterizes the maximum of its power spectral density observed in the event. The correlations between various combinations of peak values and fluences of the microwave bursts and proton enhancements are analyzed in the next section.

### 2.4. Microwave and Proton Fluences

The relations between various combinations of the peak fluxes and fluences of microwave bursts and proton enhancements are presented in Figure 4. The correlation coefficients for all events and, separately, for western events alone are shown in the upper parts of the plots. The poorly connected event 5 was treated with the correction described in Section 2.1. This increased the correlation coefficients only insignificantly (*e.g.*, $\rho_{\rm All}$ from 0.64 to 0.67 in Figure 4d).

The scatter of the data points in the top and bottom left panels is similar. The four abundant events deviate from the main cloud of points considerably less in the right panels, where the argument is $\Phi_{35}$, than in the left panels, where the argument is $F_{35}$. The main cloud of points without the four abundant events is narrower in Figure 4d than in Figure 4b. The best correspondence between the proton and microwave fluences is confirmed by the highest correlation coefficient of 0.67 for this combination of the parameters. We note that Kahler (1982) found the microwave fluences to correlate with peak proton fluxes higher than the BFS hypothesis predicted (which corresponds to our Figure 4b), but he did not consider the relation between the microwave and proton fluences (Figure 4d).

Extraordinarily high fluxes of high-energy protons were observed in four abundant mM events selected by our criteria. It is possible that these events were essentially different from the others. As Figure 4 shows, the highest correlation between the microwave and proton fluences can be due to the long duration of the abundant events. However, even for the whole set of events with $F_{35} > 1000$ sfu without the abundant events, the correlation coefficient between the fluences is 0.82 and does not exceed 0.75 for other combinations. Thus, the correlation between the microwave and proton fluences is highest in any case.

The linear fit for the whole data set is $\Phi_p = 10^{-1.99\pm1.18}\Phi_{35}^{1.12\pm0.19}$, and the correlation coefficients are $\rho_{\rm All} = 0.67$, $\rho_{\rm West} = 0.60$. The data set without the abundant mM events and atypical event 5 is fit with $\Phi_p = 10^{-4.17\pm0.96}\Phi_{35}^{1.44\pm0.15}$, and the correlation coefficients

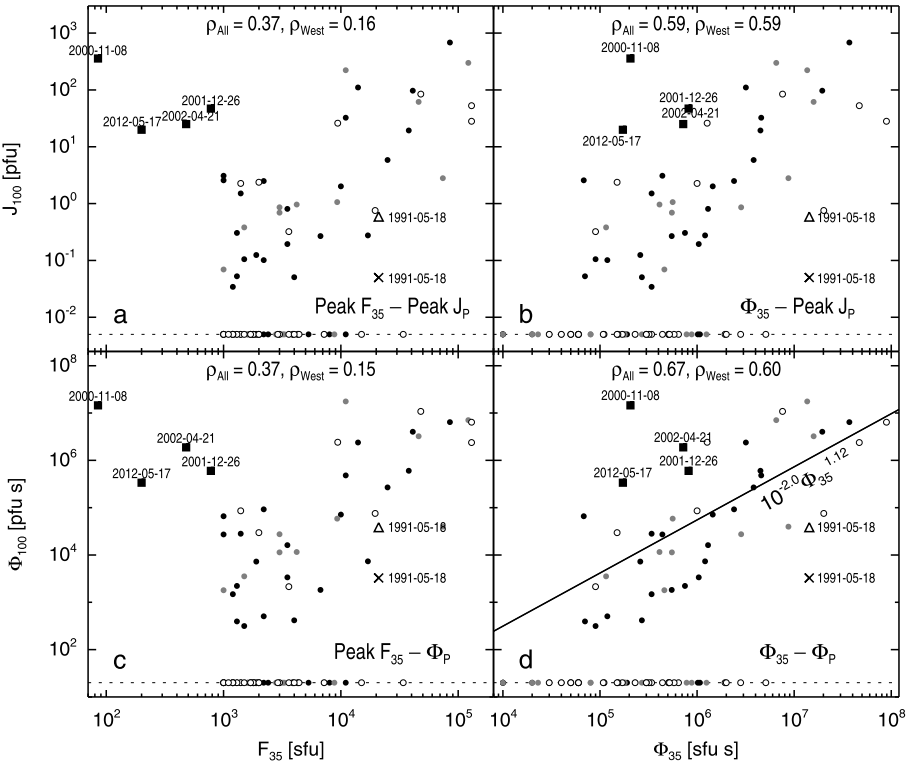


**Figure 4** Statistical relations between different combinations of the peak fluxes and fluences of microwave bursts and those of longitude-corrected SPEs. The Pearson correlation coefficients specified in each panel were calculated separately for all 44 SPEs ($\rho_{\mathrm{All}}$) and for 26 western events alone ($\rho_{\mathrm{West}}$). The meaning of the symbols is the same as in Figure 1. The line in panel (d) represents the linear fit of the (log–log) distribution. The poorly connected event on 18 May 1991 is shown both with a correction (triangle) and without it (slanted cross).

are $\rho_{\mathrm{All}} = 0.84$, $\rho_{\mathrm{West}} = 0.91$. The nonlinearity of the relation might be due to the complex dependence of the gyrosynchrotron emission on the parameters of radiating electrons, including their spectral and spatial distributions, magnetic field strength, and other factors (Dulk and Marsh, 1982; Kundu *et al.*, 2009). Our choice of a high frequency of 35 GHz simplifies the situation; the scatter at a lower frequency can be wider due to the influence of these factors.

Because the probability of a detectable > 100 MeV SPE directly depends on the peak flux and duration of a 35 GHz burst (Figure 2 and Equation (1)), its relation with the 35 GHz fluence in Figure 2 is still clearer in the histograms with nearly equal bins that cover a range of three orders of magnitude. The distributions can be approximately fitted by the empirical relations

$$\begin{aligned} P_{\mathrm{All}}(\mathrm{SPE},\ E_{\mathrm{p}} > 100\ \mathrm{MeV}) &\approx 1 - \exp\left\{-\left[\Phi_{35}/\left(1.5\times 10^{6}\right)\right]^{0.5}\right\} \\ P_{\mathrm{West}}(\mathrm{SPE},\ E_{\mathrm{p}} > 100\ \mathrm{MeV}) &\approx 1 - \exp\left\{-\left[\Phi_{35}/\left(2.7\times 10^{5}\right)\right]^{0.75}\right\}. \end{aligned} \tag{2}$$

In the future, when calibrated microwave measurements will be available in real time, these relations could be used to promptly forecast the probability and importance of nearing SPEs with an ongoing update of the quantities issued.

## 3. Origin of High-Energy SPEs

The direct relation between the microwave and proton fluences indicates the dependence of the total number of high-energy protons arriving at the Earth orbit on the total duration of the acceleration process. The correspondence between the durations of the acceleration process and the microwave burst is obvious, but it is more difficult to expect this correspondence if the protons are accelerated by shock waves far away from a flare region. Thus, the results of the preceding Section 2.4 predominantly favor a flare-related origin of the analyzed SPEs ($F_{35} \geq 10^3$ sfu) with respect to the hypothesis of their exceptional shock-acceleration. A contribution from shock-acceleration is also possible, but with a lower statistical significance – probably, in the abundant events. The suggestion is consistent with the preliminary conclusion of Trottet *et al.* (2015) that was deduced from a different approach. The authors analyzed correlations between peak proton fluxes and parameters of flares and CMEs. To additionally verify our statistical conclusions, we applied their approach to our data set.

### 3.1. Relations Between Parameters of Eruptive Solar Activity and Proton Fluences

Trottet *et al.* (2015) analyzed 44 SPEs in an energy range of 15 – 40 MeV (and corresponding fluxes of subrelativistic electrons) associated with flares of M and X GOES classes that occurred in 1997 – 2006 in the western solar hemisphere. The authors calculated correlation coefficients between logarithms of peak proton fluxes and parameters characterizing the flares and CMEs. The analyzed parameters were the peak flux of the SXR emission, start-to-peak SXR fluence, microwave fluence, and CME speed.

In the proton energy range of 15 – 40 MeV analyzed by Trottet *et al.* (2015), it is difficult to filter out the contribution from the acceleration by interplanetary shock waves far away from the Sun, which is, most likely, considerably lower for proton energies above 100 MeV. As Figure 4 and the related text show, the microwave fluence, $\Phi_{35}$, correlates with total

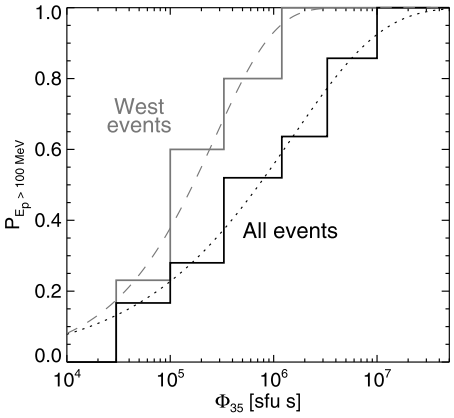


**Figure 5** Probability of a near-Earth proton enhancement with $E_P > 100$ MeV *vs.* the microwave fluence at 35 GHz irrespective of any other parameters.

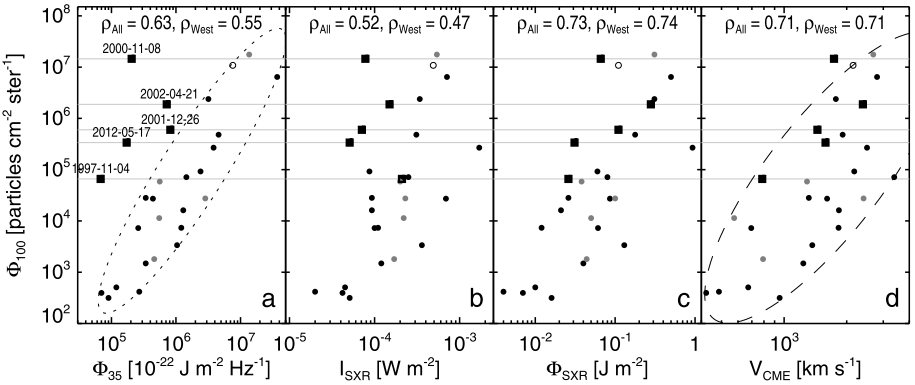


**Figure 6** Scatter (log–log) plots of longitude-corrected SPE fluence, $\Phi_{100}$, versus microwave fluence. $\Phi_{35}$, peak SXR flux, $I_{SXR}$, start-to-peak SXR fluence, $\Phi_{SXR}$, and CME speed, $V_{CME}$. The Pearson correlation coefficients specified in each panel were calculated separately for all 28 events presented ($\rho_{All}$) and for 22 western events alone ($\rho_{West}$). The meaning of the symbols is the same as in Figure 1. The gray horizontal lines trace the fluences in the abundant events. The broken ellipses in panels (a) and (d) enclose all but abundant events.

proton fluence, $\Phi_{SXR}$, considerably better than with the peak proton flux, $J_p$. Therefore, we analyze the correlations with total fluences of SPEs and not their peak fluxes.

Systematic information about CMEs and their plane-of-the-sky speeds is available in the CME catalog for events since 1996 (Yashiro *et al.*, 2004; http://cdaw.gsfc.nasa.gov/CME_list/). The speeds listed in the CME catalog are measured for the fastest feature, and therefore $V_{CME}$ for fast CMEs are most likely related to shock waves (see, *e.g.*, Ciaravella, Raymond, and Kahler, 2006). The halo shock fronts ahead of expanding fast CMEs should have shapes similar to spheroidal or elliptical ones (Grechnev *et al.*, 2011, 2013a, 2014; Kwon, Zhang, and Olmedo, 2014; Kwon, Zhang, and Vourlidas, 2015), and therefore the plane-of-the-sky speeds measured in the catalog should not be drastically different from the modules of their vectors. The CME speeds are known for 28 proton events listed in Table 1.

Figure 6 shows the logarithmic scatter plots of the proton fluence above 100 MeV with the longitudinal correction, $\Phi_{100}$, *vs.* total microwave fluence, $\Phi_{35}$ (Figure 6a); SXR peak flux, $I_{SXR}$ (Figure 6b); its start-to-peak SXR fluence, $\Phi_{SXR}$ (Figure 6c); and the CME speed, $V_{CME}$ (Figure 6d). The events without SPEs, whose logarithms are infinite, are not included in the correlation analysis. These events presented in Figure 5 should be handled using Equation (2).

The results are similar to those of Trottet *et al.* (2015). All of the scatter plots show a similar direct tendency with a scatter of the same order. Correlations in Figures 6a and 6b are considerably lower for the 22 western events with $\lambda > 20°$ than for all events because of a large contribution from the four western abundant mM events. The higher correlation of the proton fluence, $\Phi_{100}$, with SXR fluence, $\Phi_{SXR}$, than with the peak SXR flux, $I_{SXR}$, is consistent with the significance of both the intensity and duration of the acceleration process. On the other hand, a contribution from the BFS is not excluded.

Figure 6a additionally indicates that the event on 4 November 1997 (SOL1997-11-04T05:58, 51 in Table 1) probably belongs to the abundant events as well. This event was associated with a short-duration (3 min) microwave burst of up to 1000 sfu and a relatively slow CME (785 km s$^{-1}$), but its proton fluence was atypically high relative to the events with comparable microwave fluences. In its SXR peak flux of X2.1, this event is not atypi-

cal. According to its SXR fluence and the CME speed, this event resides in the upper part of the main cloud of points.

It is reasonable to assume that in the proton-abundant events, depending on their location relative to the main cloud of points in Figure 6, the contribution of shock-accelerated protons dominated. It is also possible that some additional factors were implicated, especially for the event 2000-11-08, which stands apart in Figure 6d by its abundant proton fluence, while the CME speed of 1738 $\mathrm{km\,s^{-1}}$ is insufficient to fit within the cloud of points.

Now we consider the remaining events, excluding the abundant mM events. For convenience we plot in Figures 6a and 6d the ellipses enclosing all of the non-abundant events. The ellipticity is known to visually characterize the correlation coefficient. The points inside the dotted ellipse in Figure 6a are obviously least scattered with respect to the parameters of the SXR emission and CME speed in other panels. Thus, the BFS measure referring to the SXR emission used by Kahler (1982) cannot account for the high correlation between the microwave and proton fluences. This close correlation persists over three orders of magnitude for $\Phi_{35}$ and five orders of magnitude for $\Phi_{100}$. It would be surprising if this conspicuous correspondence were an insignificant secondary effect due to BFS.

The dashed ellipse in Figure 6d characterizes the importance of the shock-acceleration according to Trottet *et al.* (2015). While almost all of the abundant events fall within the ellipse, the scatter here is obviously larger than in Figure 6a. The close correlation between $\Phi_{35}$ and $\Phi_{100}$ cannot be a result of the scattered correlation between $V_{\mathrm{CME}}$ and $\Phi_{100}$ due to the interdependence of the analyzed parameters. Thus, it cannot be caused by the BFS. For reliability, statistical characteristics of these relations are examined quantitatively in the next section.

The range of the CME speeds is one order of magnitude, being limited from below by about 400 $\mathrm{km\,s^{-1}}$, suggesting a lower limit required for CME to drive a bow shock. On the other hand, CMEs spend much energy to overcome gravity (Uralov, Grechnev, and Hudson, 2005). The gravity escape velocity at the inner boundary of the LASCO/C2 field of view, $r_{(\mathrm{C2})} = 2R_{\odot}$, is $\sqrt{2GM_{\odot}/r_{(\mathrm{C2})}} \approx 440$ $\mathrm{km\,s^{-1}}$ ($G$ the gravitational constant, $R_{\odot}$ and $M_{\odot}$ the radius and mass of the Sun). Slower CMEs, whose propelling forces cease at lesser heights (mainly from small sources), would not stretch closed structures enough to enable efficient escape of trapped flare-accelerated particles, or even fall back without any appearance in the LASCO/C2 field of view. The majority of the escaping slower CMEs is probably due to eruptions of large quiescent filaments gradually accelerating up to large distances. SPEs are not expected from such CMEs, which are too slow to produce shock waves and are not related to a flare. The lower limit for the speeds of SPE-related CMEs of about 400 $\mathrm{km\ s^{-1}}$ is expected in any case.

### 3.2. Analysis of the Correlations

To exclude secondary correlations between parameters that are not related physically, we used partial correlation coefficients, following the approach of Trottet *et al.* (2015). Unlike the classical Pearson correlation coefficients, the partial correlation coefficients reveal the individual contribution from each of the parameters, suppressing the interdependence between them. The partial correlation coefficient, $\rho_{\mathrm{j}}(\mathrm{x_j}, \mathrm{y})$, between the analyzed parameter, $\mathrm{x_j}$, and the dependent random variable, y, is calculated as the usual Pearson correlation coefficient between $\mathrm{x_j}$ and the difference $(\mathrm{y} - \mathrm{Y_j})$, where $\mathrm{Y_j}$ is the best linear fit of y, calculated from other parameters. The linear regression is used as the best-fit $\mathrm{Y_j}$:

$$\mathrm{Y_j} = \mathrm{C} + \sum_{i \neq j} x_i .$$

**Table 2** Correlations between parameters of the solar eruptive activity and SPE fluences in 28 events (1996 – 2014) in comparison with results of Trottet *et al.* (2015).

| Correlation coefficients | $\log_{10} \Phi_{100}$ | | | | $\log_{10} J_{15}$ |
|---|---|---|---|---|---|
| | All events (28) | | Without abundant events (23) | | Results of Trottet *et al.* (2015) |
| | Actual | Corrected | Actual | Corrected | |
| (1) | (2) | (3) | (4) | (5) | (6) |
| Pearson cor. coef. | | | | | |
| $\log_{10} \Phi_{35}$ | 0.58 | 0.63 | 0.89 | 0.90 | 0.67 |
| $\log_{10} I_{SXR}$ | 0.47 | 0.52 | 0.73 | 0.74 | 0.54 |
| $\log_{10} \Phi_{SXR}$ | 0.73 | 0.73 | 0.82 | 0.79 | 0.76 |
| $\log_{10} V_{CME}$ | 0.71 | 0.71 | 0.77 | 0.75 | 0.67 |
| Partial cor. coef. | | | | | |
| $\log_{10} \Phi_{35}$ | −0.02 | 0.09 | 0.59 | 0.67 | −0.10 |
| $\log_{10} I_{SXR}$ | −0.37 | −0.25 | −0.16 | 0.09 | 0.06 |
| $\log_{10} \Phi_{SXR}$ | 0.57 | 0.47 | 0.36 | 0.10 | 0.42 |
| $\log_{10} V_{CME}$ | 0.39 | 0.33 | 0.14 | 0.001 | 0.36 |
| Without $V_{CME}$ | | | | | |
| $\log_{10} \Phi_{35}$ | 0.18 | 0.27 | 0.70 | 0.74 | |
| $\log_{10} I_{SXR}$ | −0.38 | −0.27 | −0.14 | 0.10 | |
| $\log_{10} \Phi_{SXR}$ | 0.64 | 0.55 | 0.35 | 0.10 | |

The partial correlation coefficient can be considerably lower than the Pearson coefficient, but it cannot exceed it.

Table 2 presents the Pearson and partial correlation coefficients between the analyzed parameters for all 28 events (Columns 2 and 3) and for 23 events, excluding the abundant mM events (Columns 4 and 5). The correlation coefficients were calculated for both the actual proton fluences (Columns 2 and 4) and for the longitude-corrected ones (Columns 3 and 5). The Pearson correlation coefficients in the four upper rows of Column (3) correspond to Figure 6. For comparison, Column (6) lists the results obtained by Trottet *et al.* (2015) for peak proton fluxes, $J_{15}$, of a lower energy range of 15 – 40 MeV.

As Trottet *et al.* (2015) analyzed only the western events (without a longitude correction), to which both flare-related and shock-related contributions were possible, their results in Column (6) should be compared with Column (3). The Pearson correlation coefficients in these columns are similar to each other. The partial correlation coefficients in Columns (3) and (6) for $\Phi_{35}$ and $I_{SXR}$ are more distinct, while the overall conclusion of Trottet *et al.* (2015) is confirmed. The correlations between the SPEs and either the total microwave fluences or the SXR peak fluxes for all 28 events are insignificant. The correlations of high-energy proton fluences with the start-to-peak SXR fluences and the CME speeds are significant. The partial correlation coefficients of $\Phi_{100}$ with $\Phi_{SXR}$ and with $V_{CME}$ are similar to each other. Thus, our results for 28 events agree with those of Trottet *et al.* (2015).

Columns (4) and (5) present the results for the same set of events, except for the five abundant events. The Pearson correlation coefficients between the proton fluences and all independent parameters considerably increase and only weakly depend on the longitude correction. The partial correlation coefficients increase sharply for $\Phi_{35}$ and considerably reduce for $V_{CME}$. The influence of the longitude correction is strong here. The dependence on the SXR emission becomes weak, probably due to an indirect correlation via $\Phi_{35}$. These

**Table 3** Correlations between flare parameters and SPE fluences in 40 presumably flare-dominated events (1990 – 2014).

| | $\log_{10}\Phi_{100}$ | |
|---|---|---|
| | Actual | Corrected |
| Pearson correlation coefficients | | |
| $\log_{10}\Phi_{35}$ | 0.77 | 0.82 |
| $\log_{10} I_{SXR}$ | 0.66 | 0.75 |
| $\log_{10}\Phi_{SXR}$ | 0.66 | 0.74 |
| Partial correlation coefficients | | |
| $\log_{10}\Phi_{35}$ | 0.56 | 0.62 |
| $\log_{10} I_{SXR}$ | 0.33 | 0.46 |
| $\log_{10}\Phi_{SXR}$ | −0.16 | −0.15 |

circumstances apparently confirm the predominant flare origin of high-energy protons in the 23 events (Columns 4 and 5) and the major contribution from the shock-acceleration in the five abundant events. The longitudinal correction sharply decreases the significance of $\Phi_{SXR}$, probably as a result of its interdependence with $\Phi_{35}$.

We are not aware of the CME speeds for 15 proton events of 1990 – 1992 and event 54 (1998-11-22). Therefore, a rigorous analysis of the partial correlation coefficients with all of the analyzed parameters for the complete set of the 40 SPEs from 1990 to 2015 is not possible. We tried to approximately estimate the significance of the contributions from different sources by calculating the partial correlation coefficients with no account of $V_{CME}$ for the considered sets of 28 and 23 events. They are shown in the bottom three rows of Table 2. Then we compare these values with similar results obtained for all 40 events.

The partial correlation coefficients with $I_{SXR}$ in all columns and with $\Phi_{SXR}$ in Columns (4) and (5) are almost insensitive to the absence of $V_{CME}$. The largest increase shows the partial correlation coefficients with $\Phi_{35}$ in Columns (2) and (3), possibly as a result of their interdependence with $V_{CME}$. Their increase is not as large in the Columns (4) and (5), where the influence of $V_{CME}$ is weaker.

The correlation coefficients for all 40 SPEs from our list, excluding the five abundant events, are listed in Table 3. The Pearson correlation coefficients between the proton fluences and the other known parameters are not much different from the values in Columns (4) and (5) of Table 2. The partial correlation coefficients with $\Phi_{35}$ slightly decrease, but remain the largest ones. Similar to Column (5), $\Phi_{SXR}$ is insignificant, while the importance of $I_{SXR}$ sharply increases. This fact is not surprising because first, $\Phi_{35}$ is related to the total flare energy, while $I_{SXR}$ is associated with its maximum power. Both parameters can be important. Second, an indirect correlation between the proton fluence and $I_{SXR}$ through the unknown $V_{CME}$ is possible. The microwave fluence is most significant in any case.

The results lead to the following conclusions. i) The quantitative analysis of the correlation coefficients confirms the conclusions of Section 3.1. ii) The partial correlation coefficients are sensitive to the analyzed set of events and allow identifying significant parameters, but do not guarantee independence of other parameters. iii) The predominance of the flare contribution to high-energy proton enhancements in the 40 events of 1990 – 2015 with $F_{35} \geq 10^3$ sfu seems highly likely, while some contribution from shock-acceleration is not excluded in these events. iv) Similarly, the predominance of the shock-acceleration in the five abundant events seems to be quite certain, while the flare contribution in these events is not excluded.

In summary, the quantitative analysis confirms the apparent outcome from Figures 4d and 6d. The statistical predominance of the flare-related contribution to SPEs after the bursts

with $F_{35} \geq 10^3$ sfu observed during 25 years by NoRP is confirmed by the scatter plot in Figure 4d. It does not reveal conspicuous outliers, except for the five presumably shock-dominated abundant events. Some of them in the $V_{\mathrm{CME}} - \Phi_{100}$ scatter plot (Figure 6d) surpass in proton fluences their neighbors in the cloud of the points. This circumstance indicates that some factors may amplify their proton productivity.

## 4. Discussion and Conclusion

### 4.1. Results of the Analysis

The dependence of the probability of a proton enhancement on the duration of the microwave burst was analyzed and an empirical quantitative description was proposed. In contrast to the traditional estimate of the flare duration from its SXR emission, we used the duration of the microwave burst at 35 GHz, $\Delta t_{35}$. According to the Neupert effect (Neupert, 1968), $\Delta t_{35}$ should be close to the duration of the rise phase in SXR. Therefore, the difference between our estimates and the traditional way is probably not large.

Clustering the events according to the durations of the 35 GHz bursts, expected for the categories of 'impulsive' and 'gradual' events, was not revealed for the proton enhancements of $> 100$ MeV. This result might be due to the typical decrease of the microwave turnover frequency in the later phase of long-duration events that diminishes the flux density at 35 GHz. Considerable efforts were applied previously to search for a criterion or index of the flare impulsiveness (*e.g.*, Cliver *et al.*, 1989), but no certain quantitative result was obtained. Two presumable categories, differing in their particle composition and other properties, were only qualitatively distinguished in their durations. To clarify the situation, we analyzed the correlations between all combinations of the peak fluxes and fluences for the proton enhancements and the microwave bursts. For the majority of the analyzed events, the highest correlation was found between the proton fluences and the microwave and SXR fluences (Figure 6). In other words, the total number of near-Earth protons is controlled by both the intensity of the particle acceleration process and its duration. This circumstance points at a correspondence between the durations of the proton acceleration process and the flare that is obvious for the flare origin of protons, but more difficult to understand for the proton acceleration by shock waves. Thus, a probable reason for the dependence of the number of high-energy protons on the duration of an event is not a difference between the particle acceleration mechanisms, but the duration of the acceleration process.

Some conceptions of the properties of the two different categories of impulsive and gradual events might be due to the traditional idea that impulsive events are associated with confined flares and long-duration events (LDEs) are associated with eruptive flares. However, two decades of SOHO/LASCO observations have shown that this assumption was oversimplified. Indeed, most confined flares are short, and most LDEs are associated with CMEs. However, many impulsive flares are obviously eruptive, *e.g.*, events 19, 51, 55, 56, 58, 66 – 69, 90, 93, and 94 in Table 1. They include GOES X-class flares and halo CMEs. On the other hand, confined LDE flares are known, *e.g.*, some of the events in Active Region 12192 in October 2014 (Thalmann *et al.*, 2015; also, *e.g.*, event 101 in Table 1). These circumstances indicate that the duration of an event is not a reliable indicator of a dominant acceleration mechanism. In particular, one of the five presumably shock-dominated abundant events (51 in Table 1) was an impulsive one.

Recently, Reames, Cliver, and Kahler (2014) analyzed the SEP composition of 111 impulsive events with a high iron abundance and concluded that most of their sources were

associated with CMEs. It is interesting to analyze a possible overlap of the events from their list with the NoRP data which we considered. We found that the sources of 39 events from that list fell within the NoRP observation time. Four events are present in our Table 1 (56, 59, 64, and 93); weak proton enhancements above 100 MeV were observed after three of them. One major proton event (2004-11-01, 05:50) was probably due to a behind-the-limb source. The peak fluxes at 35 GHz did not exceed 100 sfu in 19 events. No bursts at 35 GHz were detectable in 16 events. Most of these events did not produce noticeable proton enhancements even in the $> 10$ MeV range.

In this respect, a direct dependence of the probability of proton enhancements on the peak intensity of microwave bursts at 35 GHz seems to deserve attention. It is important for diagnostic purposes. This dependence might be manifest at frequencies below 35 GHz, for which round-the-clock observations are more representative. The only event from the analyzed set, with a 35 GHz peak flux of $10^3$ sfu, was probably shock dominated. These facts suggest a possible indication of a dominantly flare-related source of high-energy SPE, if $F_{35} > 10^3$ sfu, or a prevailing shock-related source, if $F_{35} < 10^3$ sfu.

### 4.2. Are the Two Alternative Concepts Really Incompatible?

As mentioned, the statistical domination of flare-related acceleration of high-energy proton enhancements in most of the events, which we analyzed, does not exclude a contribution from shock-related acceleration in these events. It is supported, for example, by the analyses of the SEP composition (*e.g.*, Reames, 2009, 2013, and many others). Recent observational studies (Qiu *et al.*, 2007, Temmer *et al.*, 2010, Grechnev *et al.* 2011, 2013a) have revealed a closer association between solar eruptions, flares, shock waves, and CMEs than was previously assumed. The shock waves initially appear early in the low corona, during the rise phase of a hard X-ray and microwave burst. Particle acceleration by flare processes and shock waves can occur nearly concurrently, and therefore it is hardly possible to recognize their origin from the analysis of temporal relations or velocity dispersion. On the other hand, the account of the early appearance of shock waves at low altitudes can be helpful in the studies of the SEP acceleration by shock waves.

Conclusions about the origin of near-Earth proton enhancements made on the basis of oversimplified old hypotheses without comparing them with recent observations might be inadequate. Taking into account the results of our analysis and those of Trottet *et al.* (2015), shock-acceleration is expected to be responsible for the bulk of protons and ions accelerated to low to moderate energies. On the other hand, the major role of shock waves in the acceleration of GLE particles, which represent the SPE category with a hardest spectrum, looks questionable in events associated with powerful flares. Indeed, apparently shock-dominated non-flare-related SPEs are characterized by soft spectra (see, *e.g.*, Chertok, Grechnev, and Meshalkina, 2009; Gopalswamy *et al.*, 2015). The hardness of the proton spectra in GLE-related events is confirmed by our data set. All of these events (marked with a superscript (a) in Column (13) of Table 1) had proton indices $\delta_p < 1.5$. Protons with energies above 100 MeV are sometimes observed in non-flare-related SPEs, but their percentage is lower than in flare-related events. For example, a detailed analysis of the origin of SPE in the extreme event on 20 January 2005 that was responsible for GLE69 led Grechnev *et al.* (2008) and Klein *et al.* (2014) to the conclusions about the flare source of SPEs. Similarly, the analysis by Grechnev *et al.* (2013a) of the event on 13 December 2006 that was responsible for GLE70 revealed an inconsistency of previous arguments in favor of its exceptional shock-related source. It is possible that in exceptional non-flare-related events shock-accelerated proton fluxes are sufficient to produce a GLE under favorable conditions

**Table 4** Comparison of the proton events on 6 and 7 January 2014.

| Event | Position | GOES class | CME speed [km s$^{-1}$] | $J_{100}$ [pfu] | $J_{10}$ [pfu] | $\delta_p$ |
|---|---|---|---|---|---|---|
| SOL2014-01-06T07:50 | S15W113 | $\approx$ X2 | 1402 | 4 | 40 | 1.00 |
| SOL2014-01-07T18:32 | S11W11 | X1.2 | 1830 | 4 | 900 | 2.35 |

(Cliver, 2006). However, it is difficult to expect that if a powerful flare occurs, then shock-accelerated protons provide the main contribution to the GLE, relative to the flare-related contribution dominating at high energies. We analyzed the GOES integral proton channel above 100 MeV, although particles of much higher energies, $\gtrsim 1$ GeV, are responsible for GLEs.

These considerations seem to be challenged in a recent study of Thakur *et al.* (2014), where the authors came to a conclusion about exceptional shock-related origin of the GLE on 6 January 2014. It was produced by a behind-the-limb SOL2014-01-06 event in Active Region 11936 (Table 4), where the STEREO telescopes recorded a powerful flare with an estimated GOES importance of about X2 (Chertok, Belov, and Grechnev, 2015). Proceeding from the remoteness of the flare region from the well-connected longitudes (like event 110 in Table 1 associated with GLE61 on 18 April 2001), Thakur *et al.* (2014) stated that this event, as well as other GLEs from behind-the-limb sources, posed a challenge to the flare acceleration mechanism for GLE particles. However, as the facts and speculations in the preceding paragraph show, the shock-related origin of some GLEs does not contradict a major flare contribution to the others.

Assuming a direct escape of flare-accelerated protons into the interplanetary space from the active region core in the low corona, Thakur *et al.* (2014) pointed out that the flare-accelerated particles would need to interact with the CME flux-rope to reach the well-connected field lines, and thus their scattering would not allow the high anisotropy typical of the beginning of the GLEs. It is difficult to agree with this argument because the main cause of the anisotropy of GLE particles is their transport in the interplanetary space. There are some other complicating factors such as the perpendicular diffusion that is difficult to take into account in simple considerations. A surprising example presents an SPE caused by the event on 1 September 2014 behind the eastern limb, when the rise phase during half a day was dominated by $> 100$ MeV protons. Furthermore, there is a possibility that accelerated protons are trapped in the CME flux-rope trap (similar to electrons responsible for type IV radio bursts) and that they are confined until reconnection of the flux rope with an open magnetic structure such as a coronal hole or streamer that allows the trapped particles access to the interplanetary space (see, *e.g.*, Masson *et al.*, 2012; Grechnev *et al.*, 2013b). In this case, the escape conditions for protons accelerated in a flare and at the shock front ahead of a CME are practically the same.

It is useful to compare the event on 6 January with another, which occurred on the next day, 7 January 2014 (Table 4), in Active Region 11944 on the Earth-facing solar side. This also produced an SPE, but not a GLE. The peak flux of $> 100$ MeV protons was the same as on 6 January, while the lower-energy SPE was stronger and longer. The 7 January CME was considerably faster than the 6 January CME. The peak flux of the gyrosynchrotron emission of 2500 sfu occurred on 7 January at about 5 GHz. All of the GLE-related events from our sample had a higher turnover frequency (Grechnev *et al.*, 2013b); parameters of the microwave emission on 6 January are unknown. The relation between the parameters of the two events is not surprising if the softer shock-related SPE component that dominated lower

energies was stronger on 7 January, while the harder flare-related component that dominated higher energies was stronger on 6 January. Otherwise, the relation seems to be challenging. For all of the listed reasons, the arguments against the flare-related source of the GLE on 6 January 2014 are not convincing.

The existence of the two concurrent different sources of accelerated protons has been argued previously in several studies mentioned in Section 1. This alternative to the single-source hypothesis invoked by Kahler (1982) can also be checked by comparing the peak-size distributions of SPEs and all flares. Analyzing the differential distribution functions *vs.* energy, Hudson (1978) concluded that the proton production was more efficient in more energetic flares. Three decades later, Belov *et al.* (2007) have analyzed detailed distributions based on much richer data. They demonstrated that the slope of the distribution of SPE-related flares was flatter than that of all flares at their low-to-moderate GOES importance (*i.e.*, the SPE productivity of weaker events was less dependent on the SXR peak flux). For larger flares, the slope of SPE-related flares approached that of all flares. These circumstances also confirm the existence of the two sources of SPEs; one, shock-related, dominates in events with weaker flares, and the second, flare-related, dominates in stronger flares. We note that the analyses of the peak-size distributions did not consider the event duration whose role we discussed (Hudson, 1978 also admitted this possibility).

All of the listed facts indicate that the role of the BFS was most likely overestimated by Kahler (1982). He stated a higher correlation between the 8.8 and 15.4 GHz fluences and SPE peak fluxes than the BFS could provide, but did not consider this correlation to be important, having failed to find any correspondence between the spectral parameters of SPEs and microwaves (a similar conclusion was made about hard X-rays). Some aspects of this correspondence have been revealed later. Chertok, Grechnev, and Meshalkina (2009) demonstrated the statistical correspondence between $\delta_{\mathrm{p}}$ and spectral parameters of microwave bursts. Grechnev *et al.* (2013b) showed that the SPEs produced in events with $F_{35} > 10^3$ sfu were harder than those after weaker bursts. The results of Kahler (1982) might be determined by the limitations of the microwave data used in his analysis. Most of the 50 events he analyzed had peak microwave fluxes from $10^2$ to $10^4$ sfu in the whole frequency range; only two were stronger. When referred to 35 GHz, the majority of these events fall into the mM category, suggestive of prevailing shock-acceleration of SPEs, as we showed. Thus, the extension of our results to SPEs associated with weaker microwave bursts probably mainly correspond to the results of Kahler (1982).

### 4.3. Concluding Remarks

Our analysis has not revealed a separation of the analyzed data set at 35 GHz according to their durations into the clusters of impulsive and gradual events. Relations were established between the intensities and durations of microwave bursts and the probability of near-Earth proton enhancements with energies $> 100$ MeV. Most likely, the causes of these dependencies are related to propagation effects of protons from their solar sources to Earth and the limited sensitivity of the detectors. This circumstance suggests the possibility that protons are accelerated to high energies in all flares accompanied by sufficiently strong bursts at 35 GHz, *i.e.*, whenever very many electrons are accelerated to relativistic energies. This indication corresponds to the conclusions of Livshits and Belov (2004) about the simultaneous acceleration of electrons and protons.

Our results are consistent with the main conclusion of Trottet *et al.* (2015) and confirm their suggestion that the flare acceleration dominates for high-energy protons. For the majority of the analyzed events, we found a direct dependence with a high correlation between the

parameters of the flare and proton fluences $> 100$ MeV. Comparable correlations between the proton fluences with start-to-peak SXR fluences and microwave emission show that both these parameters characterizing solar flares can be used for the diagnostics of proton enhancements, and their importance is not diminished by the Big Flare Syndrome hypothesis. Comparison of Figures 1a, 1b, 4d, and Table 3 demonstrates that finding and accounting for the factors that affect the quantitative parameters of near-Earth proton enhancements allows a considerably reduction of the uncertainty of their expected values that is evaluated by a conspicuous increase of the correlation coefficients. Perhaps some other affecting factors exist, which, if accounted for, would additionally reduce the scatter. For example, by using a combination of the peak flux, effective duration, and the turnover frequency of the microwave bursts, Isaeva, Melnikov, and Tsvetkov (2010) reached a considerably higher correlation with SPE parameters.

A detailed analysis of recent observational data promises a substantial progress in understanding the sources of near-Earth proton enhancements and their prompt forecast. It seems worthwhile to analyze the events in which the contribution from only one of the two competing sources of accelerated protons is most probable. We note, however, that according to recent observational studies, shock waves develop in the low corona during flares and the early formation of CMEs. This update can help in studies of particle acceleration by shock waves, but it makes recognizing the sources of SPEs still more difficult. Most likely, events with exceptional flare-acceleration do not exist because shock waves develop even in eruptive events without detectable microwave bursts, while the escape of accelerated protons from confined flares is hampered. On the other hand, SPEs without powerful flares but with strong shock waves are known. Case studies of the latter events might shed more light on one of the two sources of SPEs. The results of these studies would provide guidelines for future statistical analyses.

**Acknowledgements** We thank A.V. Belov, B.Yu. Yushkov, V.G. Kurt, M.A. Livshits, H. Nakajima, K.-L. Klein, N.V. Nitta, V.E. Sdobnov, V.F. Melnikov, V.V. Zharkova, and S.S. Kalashnikov for useful discussions and assistance. We thank the anonymous referee for valuable comments. We are grateful to the instrumental teams operating *Nobeyama Radio Polarimeters* and GOES satellites for the data used here. The CME Catalog used in this article is generated and maintained at the CDAW Data Center by NASA and the Catholic University of America in cooperation with the Naval Research Laboratory. SOHO is a project of international cooperation between ESA and NASA. The authors thank the CDAW Team for the data. This study was supported by the Russian Foundation of Basic Research under grants 14-02-00367, 15-02-10036, and 15-02-01089, by the Russian Science Foundation under grant 16-12-00019, and the Program of basic scientific research of RAS No. II.16.1.6. N.M. was partly supported by the Marie Curie PIRSES-GA-2011-295272 RadioSun project.

## References

Akinian, S.T., Alibegov, M.M., Kozlovski, V.D., Chertok, I.M.: 1978, *Geomagn. Aeron.* **18**, 410.
Aschwanden, M.J.: 2012, *Space Sci. Rev.* **173**, 3. DOI.
Belov, A.V.: 2009, *Adv. Space Res.* **43**, 467. DOI.
Belov, A., Kurt, V., Mavromichalaki, H., Gerontidou, M.: 2007, *Solar Phys.* **246**, 457. DOI.
Brueckner, G.E., Howard, R.A., Koomen, M.J., Korendyke, C.M., Michels, D.J., Moses, J.D., Socker, D.G., Dere, K.P., Lamy, P.L., Llebaria, A., *et al.*: 1995, *Solar Phys.* **162**, 357. DOI.
Castelli, J.P., Barron, W.R.: 1977, *J. Geophys. Res.* **82**, 1275. DOI.
Chertok, I.M.: 1990, *Astron. Nachr.* **311**, 379. DOI.
Chertok, I.M., Grechnev, V.V., Meshalkina, N.S.: 2009, *Astron. Rep.* **86**, 1133. DOI.
Chertok, I.M., Belov, A.V., Grechnev, V.V.: 2015, *Solar Phys.* **290**, 1947. DOI.
Chupp, E.L., Ryan, J.M.: 2009, *Res. Astron. Astrophys.* **9**, 11. DOI.
Ciaravella, A., Raymond, J.C., Kahler, S.W.: 2006, *Astrophys. J.* **652**, 774. DOI.
Cliver, E.W.: 2006, *Astrophys. J.* **639**, 1206. DOI.

Cliver, E.W., Forrest, D.J., Cane, H.V., Reames, D.V., McGuire, R.E., von Rosenvinge, T.T., Kane, S.R., MacDowall, R.J.: 1989, *Astrophys. J.* **343**, 953. DOI.
Croom, D.L.: 1971, *Solar Phys.* **19**, 171. DOI.
Dierckxsens, M., Tziotziou, K., Dalla, S., Patsou, I., Marsh, M.S., Crosby, N.B., Malandraki, O., Tsiropoula, G.: 2015, *Solar Phys.* **290**, 841. DOI.
Dulk, G.A., Marsh, K.A.: 1982, *Astrophys. J.* **259**, 350. DOI.
Gopalswamy, N., Xie, H., Yashiro, S., Usoskin, I.: 2005, In: Sripathi, B., *et al.* (eds.) *Proc. 29th Int. Cosmic Ray Conf.* **1**, Tata Institute of Fundamental Research, Mumbai, 169.
Gopalswamy, N., Xie, H., Yashiro, S., Akiyama, S., Mäkelä, P., Usoskin, I.G.: 2012, *Space Sci. Rev.* **171**, 23. DOI.
Gopalswamy, N., Mäkelä, P., Akiyama, S., Yashiro, S., Xie, H., Thakur, N., Kahler, S.W.: 2015, *Astrophys. J.* **806**, 8. DOI.
Grechnev, V.V., Kurt, V.G., Chertok, I.M., Uralov, A.M., Nakajima, H., Altyntsev, A.T., Belov, A.V., Yushkov, B.Y., Kuznetsov, S.N., Kashapova, L.K., Meshalkina, N.S., Prestage, N.P.: 2008, *Solar Phys.* **252**, 149. DOI.
Grechnev, V.V., Uralov, A.M., Chertok, I.M., Kuzmenko, I.V., Afanasyev, A.N., Meshalkina, N.S., Kalashnikov, S.S., Kubo, Y.: 2011, *Solar Phys.* **273**, 433. DOI.
Grechnev, V.V., Kiselev, V.I., Uralov, A.M., Meshalkina, N.S., Kochanov, A.A.: 2013a. *Publ. Astron. Soc. Japan* **65**(SP1), S9. DOI.
Grechnev, V.V., Meshalkina, N.S., Chertok, I.M., Kiselev, V.I.: 2013b. *Publ. Astron. Soc. Japan* **65**(SP1), S4. DOI.
Grechnev, V.V., Uralov, A.M., Chertok, I.M., Slemzin, V.A., Filippov, B.P., Egorov Ya, I., Fainshtein, V.G., Afanasyev, A.N., Prestage, N., Temmer, M.: 2014, *Solar Phys.* **289**, 1279. DOI.
Grechnev, V.V., Uralov, A.M., Kuzmenko, I.V., Kochanov, A.A., Chertok, I.M., Kalashnikov, S.S.: 2015, *Solar Phys.* **290**, 129. DOI.
Hudson, H.S.: 1978, *Solar Phys.* **57**, 237. DOI.
Isaeva, E.A., Melnikov, V.F., Tsvetkov, L.I.: 2010, *Bull. Crimean Astrophys. Obs.* **106**, 26. DOI.
Kahler, S.W.: 1982, *J. Geophys. Res.* **87**, 3439. DOI.
Kallenrode, M.-B.: 2003, *J. Phys. G* **29**, 965.
Klein, K.-L., Masson, S., Bouratzis, C., Grechnev, V., Hillaris, A., Preka-Papadema, P.: 2014, *Astron. Astrophys.* **572**, AA4. DOI.
Kundu, M.R., Grechnev, V.V., White, S.M., Schmahl, E.J., Meshalkina, N.S., Kashapova, L.K.: 2009, *Solar Phys.* **260**, 135. DOI.
Kurt, V., Belov, A., Mavromichalaki, H., Gerontidou, M.: 2004, *Ann. Geophys.* **22**, 2255. DOI.
Kwon, R.-Y., Zhang, J., Olmedo, O.: 2014, *Astrophys. J.* **794**, 148. DOI.
Kwon, R.-Y., Zhang, J., Vourlidas, A.: 2015, *Astrophys. J. Lett.* **799**, L29. DOI.
Lario, D., Aran, A., Gómez-Herrero, R., Dresing, N., Heber, B., Ho, G.C., Decker, R.B., Roelof, E.C.: 2013, *Astrophys. J.* **767**, 41. DOI.
Livshits, M.A., Belov, A.V.: 2004, *Astron. Rep.* **48**, 665. DOI.
Masson, S., Aulanier, G., Pariat, E., Klein, K.-L.: 2012, *Solar Phys.* **276**, 199. DOI.
Melnikov, V.F., Podstrigach, T.S., Dajbog, E.I., Stolpovskij, V.G.: 1991, *Cosm. Res.* **29**, 87.
Miklenic, C.H., Veronig, A.M., Vršnak, B.: 2009, *Astron. Astrophys.* **499**, 893. DOI.
Nakajima, H., Sekiguchi, H., Sawa, M., Kai, K., Kawashima, S.: 1985, *Publ. Astron. Soc. Japan* **37**, 163.
Nakajima, H., Nishio, M., Enome, S., Shibasaki, K., Takano, T., Hanaoka, Y., Torii, C., Sekiguchi, H., *et al.*: 1994, *Proc. IEEE* **82**, 705.
Neupert, W.M.: 1968, *Astrophys. J. Lett.* **153**, L59. DOI.
Nitta, N.V., Cliver, E.W., Tylka, A.J.: 2003, *Astrophys. J. Lett.* **568**, L103. DOI.
Qiu, J., Hu, Q., Howard, T., Yurchyshyn, V.: 2007, *Astrophys. J.* **659**, 758. DOI.
Reames, D.V.: 2009, *Astrophys. J.* **693**, 812. DOI.
Reames, D.V.: 2013, *Space Sci. Rev.* **175**, 53. DOI.
Reames, D.V., Cliver, E.W., Kahler, S.W.: 2014, *Solar Phys.* **289**, 3817. DOI.
Rouillard, A.P., Sheeley, N.R., Tylka, A., Vourlidas, A., Ng, C.K., Rakowski, C., Cohen, C.M.S., Mewaldt, R.A., Mason, G.M., Reames, D., Savani, N.P., StCyr, O.C., Szabo, A.: 2012, *Astrophys. J.* **752**, 44. DOI.
Sladkova, A.I., Bazilevskaya, G.A., Ishkov, V.N., Nazarova, M.N., Pereyaslova, N.K., Stupishin, A.G., Ulyev, V.A., Chertok, I.M.: 1998, In: Logachev, Yu.I. (ed.) *Catalogue of Solar Proton Events 1987–1996*, Moscow University Press, Moscow, 41, 137, and 223
Temmer, M., Veronig, A.M., Vršnak, B., Rybák, J., Gömöry, P., Stoiser, S., Maričić, D.: 2008, *Astrophys. J.* **673**, 95. DOI.
Temmer, M., Veronig, A., Kontar, E., Krucker, S., Vršnak, B.: 2010, *Astrophys. J.* **712**, 1410. DOI.
Thakur, N., Gopalswamy, N., Xie, H., Mäkelä, P., Yashiro, S., Akiyama, S., Davila, J.M.: 2014, *Astrophys. J. Lett.* **790**, L13. DOI.

Thalmann, J.K., Su, Y., Temmer, M., Veronig, A.M.: 2015, *Astrophys. J. Lett.* **801**, L23. DOI.
Trottet, G., Samwel, S., Klein, K.-L., Dudok de Wit, T., Miteva, R.: 2015, *Solar Phys.* **290**, 819. DOI.
Tylka, A.J., Cohen, C.M.S., Dietrich, W.F., Lee, M.A., Maclennan, C.G., Mewaldt, R.A., Ng, C.K., Reames, D.V.: 2005, *Astrophys. J.* **625**, 474. DOI.
Uralov, A.M., Grechnev, V.V., Hudson, H.S.: 2005, *J. Geophys. Res., Atmos.* **110**, A05104. DOI.
Vilmer, N., MacKinnon, A.L., Hurford, G.J.: 2011, *Space Sci. Rev.* **159**, 167. DOI.
Yashiro, S., Gopalswamy, N., Michalek, G., St. Cyr, O.C., Plunkett, S.P., Rich, N.B., Howard, R.A.: 2004, *J. Geophys. Res.* **109**, A07105. DOI.
Zhang, J., Dere, K.P., Howard, R.A., Kundu, M.R., White, S.M.: 2001, *Astrophys. J.* **559**, 452. DOI.